

Tacrine–Ferulic Acid–Nitric Oxide (NO) Donor Trihybrids as Potent, Multifunctional Acetyl- and Butyrylcholinesterase Inhibitors

Yao Chen,^{†,‡,§} Jianfei Sun,^{||} Lei Fang,[‡] Mei Liu,^{||} Sixun Peng,^{†,‡} Hong Liao,^{*,||} Jochen Lehmann,^{*,§,⊥} and Yihua Zhang^{*,†,‡}

[†]State Key Laboratory of Natural Medicines, China Pharmaceutical University, Nanjing 210009, PR China

[‡]Center of Drug Discovery, China Pharmaceutical University, Nanjing 210009, PR China

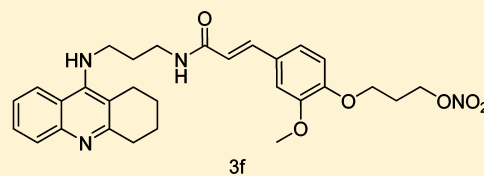
[§]Lehrstuhl für Pharmazeutische/Medizinische Chemie, Institut für Pharmazie, Friedrich-Schiller-Universität Jena, Philosophenweg 14, D-07743 Jena, Germany

^{||}Neurobiology Lab, New Drug Screening Center, China Pharmaceutical University, Nanjing 210009, P.R. China

[⊥]College of Pharmacy, King Saud University Riyadh, Saudi Arabia

S Supporting Information

ABSTRACT: In search of multifunctional cholinesterase inhibitors as potential anti-Alzheimer drug candidates, tacrine–ferulic acid–NO donor trihybrids were synthesized and tested for their cholinesterase inhibitory activities, release of nitric oxide, vasodilator properties, cognition improving potency, and hepatotoxicity. All of the novel target compounds show higher in vitro cholinesterase inhibitory activity than tacrine. Three selected compounds (**3a**, **3f**, and **3k**) produce moderate vasorelaxation in vitro, which correlates with the release of nitric oxide. Compared to its non-nitrate dihybrid analogue (**3u**), the trihybrid **3f** exhibits better performance in improving the scopolamine-induced cognition impairment (mice) and, furthermore, less hepatotoxicity than tacrine.



(IC₅₀ for AChE = 10.9 nM; IC₅₀ for BuChE = 17.7 nM)

■ INTRODUCTION

The cholinergic hypothesis of the pathogenesis of Alzheimer's disease (AD)¹ asserts that dysfunction of cholinergic system, mainly decline of acetylcholine (ACh) level, leads to the cognitive and memory deficits associated with AD, and sustaining or recovering cholinergic function is therefore supposed to be clinically beneficial.^{2,3} ACh can be degraded by two types of cholinesterases (ChEs), namely acetylcholinesterase (AChE) and butyrylcholinesterase (BuChE). The enzymatic cavity of human AChE has the shape of a nearly 20 Å deep narrow gorge^{4,5} which is composed of two binding sites: the catalytic active site (CAS) at the bottom and the peripheral anionic site (PAS) near the entrance of the gorge.^{6–8} PAS has been proved to have close relation to both hydrolysis of ACh and neurotoxic cascade of AD through AChE-induced β -amyloid ($A\beta$) aggregation.^{9–11} Human BuChE has a similar structure of the cavity but with a wider gorge.^{12,13} Compared to BuChE, AChE is more active and can hydrolyze most of ACh (80% according to Carolan, C. G., et al. and Arce, M. P., et al.) in normal brains.¹⁴ However, in the case of AD, both the level and the activity of AChE are found to be significantly reduced, whereas BuChE is increased and modulates the ACh levels.^{15,16} Consequently, not only AChE but both enzymes are important targets in the therapy of AD,¹⁷ and inhibitors of both, such as tacrine (Figure 1) and rivastigmine, have been clinically applied. Unfortunately, instead of curing or preventing the neurodegeneration, cholinesterase inhibitors (ChEIs) only enable a

palliative treatment.¹⁸ Because of the multifactorial nature of AD, the traditional approach of single-target molecule can generally only offer limited and transient benefits. Thus, a strategy named multitarget-directed ligands (MTDLs)¹⁹ has recently been applied in the research of ChEIs,^{20,21} which means compounds with additional properties other than cholinesterase inhibition have been focused. To extend this strategy and further explore its potential is the topic of this work.

Nitric oxide (NO), a free radical gas, is a multifunctional messenger molecule with diverse physiological roles, such as dilation of blood vessels, immune responses, and potentiation of synaptic transmission.^{22,23} Although the relation between NO and AD is not yet clear, increasing recent evidence suggests that NO may be beneficial for the treatment of AD also by increasing blood supply²⁴ and regulating the cerebral circulation.²⁵ In recent years, in the research of anti-AD drugs, the NO-donating compound strategy,²⁶ in which a NO-donor is combined to a "native" molecule, has been proved to be effective.^{27–29}

Previously, we have reported on several tacrine–ferulic acid hybrids (**1a–d**, Figure 1) as potent ChEIs which can block the PAS³⁰ and on highly active and nontoxic tacrine–organic nitrate (**2**, Figure 1).^{28,31} To obtain new multifunctional ChEIs

Received: January 25, 2012

Published: April 18, 2012

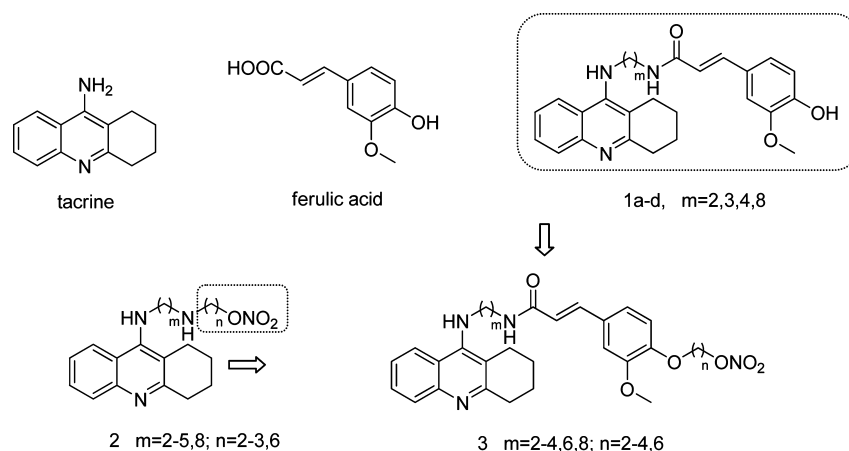


Figure 1. Structures of tacrine, previous tacrine hybrid compounds 1a–d and 2, and tacrine trihybrid compounds 3a–t designed for this study.

endowed with additional properties at least such as vessel relaxation activity, a nitrate moiety was conjugated to the tacrine–ferulic acid hybrid compounds, via alkylenediamine side chain, leading to a series of novel trihybrids 3a–t.

In the present study, we describe the synthesis and pharmacological evaluation of novel potential anti-Alzheimer compounds. The pharmacological evaluation includes AChE and BuChE inhibition, the kinetics of enzyme inhibition, NO-releasing test, vascular relaxation study, in vivo behavioral study, and hepatotoxicity studies.

RESULTS AND DISCUSSION

Chemistry. The synthesis of the NO-donating tacrine–ferulic acid hybrids and related compounds was depicted in Scheme 1. 9-Aminoalkylamino-1,2,3,4-tetrahydroacridines 10a–e were synthesized starting from anthranilic acid, which was condensed with cyclohexanone to yield chloro acridine 9.³² Treatment of 9 with corresponding alkylenediamines resulted in 10a–e. Ferulic acid was esterified to give methyl ester 5, which was treated with dibromoalkanes to give bromo compounds 6a–d, followed by treatment of AgNO₃ in dry CH₃CN to offer nitrates 7a–d. The nitrates were demethylated under basic conditions to yield acids 8a–d, which were coupled with 10a–e in the presence of DCC/DMAP to provide target compounds 3a–t. Treatment of 5 with 1-bromopropane gave propylated compound 6e and 8e by hydrolytic cleavage. Condensation of 8e with 10b led to compound 3u. In addition, ferulic acid was directly coupled with 10d to generate compound 4.

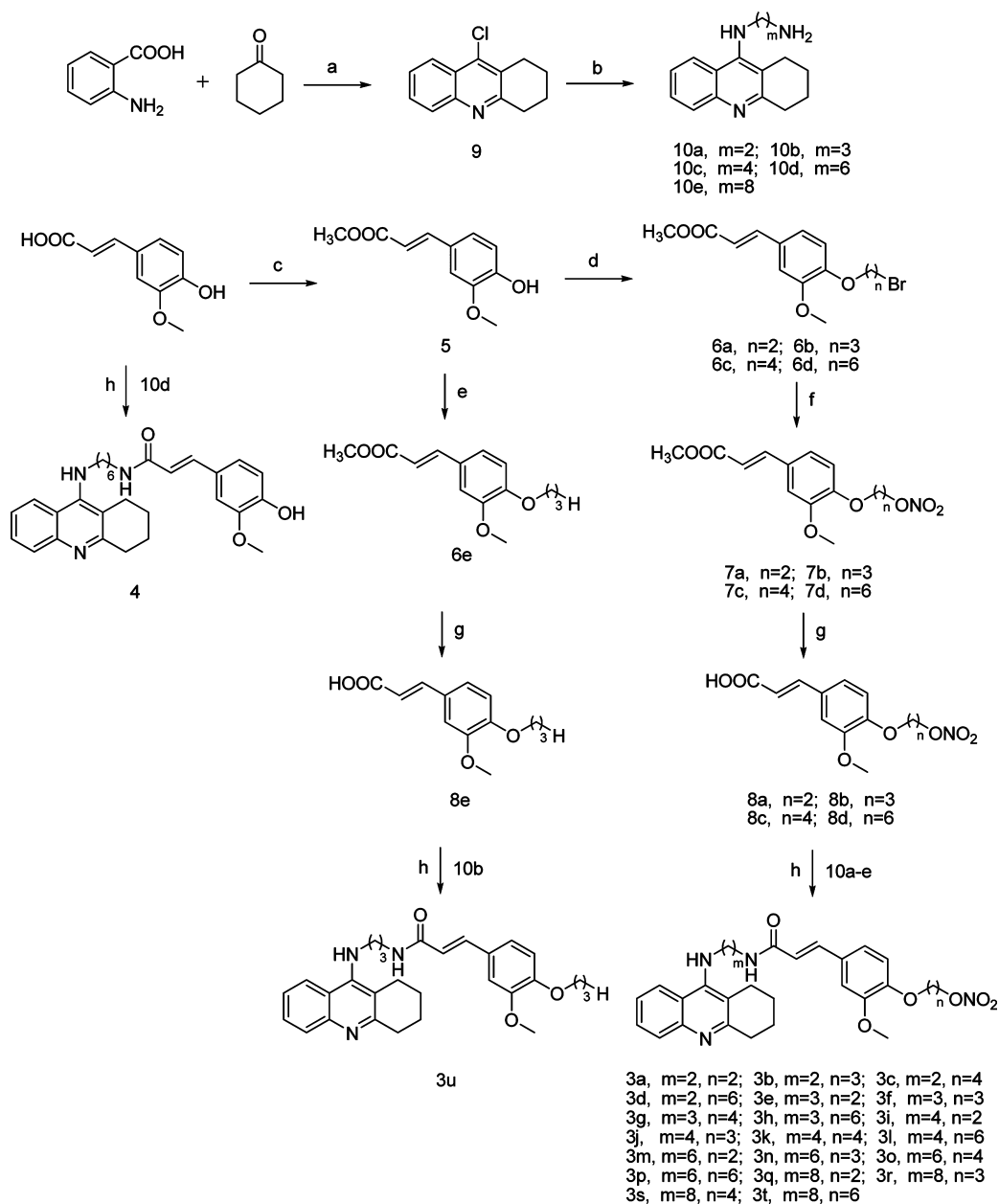
Pharmacology. *AChE and BuChE Inhibition.* The hybrids 3a–t and relative compounds were evaluated in vitro as inhibitors of AChE from *Electrophorus electricus* (eeAChE) and of BuChE from equine serum, following Ellman's method³³ (Table 1). The inhibitory activities of the hybrids were compared to those of tacrine, 1a–d and 4, as well as to the free amine precursors 10a–e and the ferulic acid derivatives 8a–d. All of the novel target compounds proved to be very potent inhibitors of both cholinesterases. The results of 10a–e showed a trend consistent with the target compounds, whereas 8a–d showed quite low affinity, indicating the tacrine analogue moiety as the key structure for the ChE inhibitory activity. In addition, the results revealed that the length of the diamine side chain attached to the tacrine skeleton of the hybrids markedly influenced the ability to inhibit ChE, and the optimal spacer length was 6–8 atoms. Moreover, the target compounds 3a–t

showed better or comparable activity compared to the corresponding parent compounds 1a–d and 4, indicating that the introduction of nitrate group might be a contribution to the inhibitory activity. Particularly, 3u, an analogue of 3f without the nitrate group, showed lower activity (IC₅₀ of AChE = 69.8 nM; IC₅₀ of BuChE = 40.3 nM) than the parent compound 1b (IC₅₀ of AChE = 56.7 nM; IC₅₀ of BuChE = 31.1 nM) and 3f (IC₅₀ of AChE = 10.9 nM; IC₅₀ of BuChE = 17.7 nM), which demonstrated that the alkane linker itself made no contribution to the activity, highlighting the importance of the nitrate group for the ChE inhibition.

Kinetic Study of ChE Inhibition. To gain information on the mechanism of inhibition, the potent inhibitor 3f was selected for a kinetic study. This compound 3f was chosen not only for kinetic studies but also for the further behavioral and hepatotoxicity studies because of being the best candidate in total performance with regard to cholinesterase inhibition, release of NO, and vasodilatation. The type of inhibition was elucidated from the analysis of Lineweaver–Burk reciprocal plots, which were reciprocal rates versus reciprocal substrate concentrations for the different inhibitor concentrations resulting from the substrate–velocity curves for ChEs. For AChE, the plot showed both increased slopes (decreased V_{max}) and intercepts (higher K_m) at increasing concentration of the inhibitor (Figure 2). This pattern indicated a mixed-type inhibition and therefore supported the dual site (CAS and PAS) binding of these compounds. In contrast, a different plot for BuChE was obtained, showing different K_m and constant V_{max} in different inhibitor concentrations (Figure 3). This suggested a competitive inhibition, revealing that these compounds compete for the same binding site (CAS) as the substrate acetylcholine.

Antioxidant Activities. Target compounds (3a–t and 4) were tested for the antioxidant activity using a radical scavenging assay (DPPH assay).³⁴ However, all the target compounds (except compound 4) showed no antioxidant activities (at concentration 2 mM, the free radical scavenging activities in % of compounds 3a–t were less than 1%, while of compound 4 was 64.7%, compared to reference ferulic acid 100%). Very probably, these results are due to the presence or absence of the free phenolic hydroxy groups of ferulic acid in these prodrug-hybrid compounds.

Correlation of NO Produced by the Hybrids with Their Vascular Relaxation Activities. To investigate the potential relationship between the NO generated or at least mimicked by

Scheme 1. Synthesis of Compounds 3a–u and 4^a

^aReagents: (a) POCl₃, reflux, 3 h; (b) pentanol, NH₂(CH₂)_mNH₂, reflux, 18 h; (c) CH₃OH, H₂SO₄, reflux, 3 h; (d) Br(CH₂)_nBr, DMF, K₂CO₃, 65 °C, 6 h; (e) Br(CH₂)₂CH₃, DMF, K₂CO₃, 65 °C, 6 h; (f) AgNO₃, CH₃CN, 60 °C, 6 h; (g) LiOH, THF/CH₃OH/H₂O, room temp, 24 h; (h) DCC, DMAP, anhydrous CH₂Cl₂, room temp, 24 h.

the target compounds and their vasodilator activities, the in vitro reactivity of compounds 3a–t as NO-donating compounds was first measured using the Griess reaction³⁵ which quantifies the inorganic nitrite produced from the degradation of the organic nitrate (Table 1). Of course, all the compounds showed higher levels of nitrite than tacrine, and compound 3f and 3q produced levels of nitrite (0.31, 0.30 μg/mL, respectively) near to the positive control isosorbide dinitrate (ISDN, 0.38 μg/mL).

Compounds 1b, 3a, 3f, 3q, and 3u were evaluated in an ex vivo organ bath (coronary arteries from rat) vascular relaxation assay. ISDN and tacrine were taken as positive and negative controls, respectively (Figure 4). All the tested compounds (except 1b) showed higher activity than tacrine, and 3f showed

a comparable EC₅₀ (34.3 μM) to ISDN (EC₅₀ = 25.2 μM). The activity of parent compound 1b was quite low due to the lack of NO donor. The comparison between 3f and 3u confirms that the nitrate group is crucial to the vascular relaxation potency. Moreover, the levels of NO produced by the target compounds are positively correlated with the vasorelaxation effects with the exception of 3q.

To study the unexpected result of this compound, we detected the levels of nitrite generated by 3f and 3q after different times (10, 30, and 90 min, respectively). The results (Figure 5) demonstrate that, the NO releasing rate of 3q lower in the beginning, which should explain the lower vasorelaxation effect of 3q because this activity was determined 5 min after the test compounds were added.

Table 1. Inhibition of AChE and BuChE (IC_{50} Values), Selectivity Expressed as the Ratio of the Resulting IC_{50} Values and Release of nitrite from the organic nitrates measured by Griess reaction

compd	IC_{50} (nM) \pm SEM ^a		selectivity ratio ^b	nitrite (μ g/mL) ^c
	AChE	BuChE		
1a	62.0 \pm 10.5	37.5 \pm 9.7	1.7	nd ^d
1b	56.7 \pm 14.4	31.1 \pm 4.8	1.8	nd
1c	11.1 \pm 1.8	9.8 \pm 1.8	1.1	nd
1d	16.9 \pm 3.4	27.4 \pm 8.3	0.6	nd
10a	71.4 \pm 11.0	30.9 \pm 11.2	2.3	nd
10b	79.5 \pm 14.3	19.7 \pm 2.9	4.1	nd
10c	39.3 \pm 5.1	22.9 \pm 2.4	1.7	nd
10d	23.7 \pm 5.7	6.6 \pm 0.5	3.6	nd
10e	2.9 \pm 1.0	2.8 \pm 0.4	1.0	nd
8a	>10000	>10000		nd
8b	>10000	>10000		nd
8c	>10000	>10000		nd
8d	>10000	>10000		nd
3a	17.2 \pm 2.3	10.5 \pm 1.1	1.6	0.182 \pm 0.003
3b	19.9 \pm 5.0	8.4 \pm 1.1	2.4	0.071 \pm 0.003
3c	27.1 \pm 2.6	7.6 \pm 0.9	3.6	0.042 \pm 0.003
3d	40.6 \pm 2.8	21.8 \pm 1.7	1.9	0.221 \pm 0.002
3e	14.4 \pm 2.2	24.9 \pm 2.4	0.6	0.243 \pm 0.001
3f	10.9 \pm 1.3	17.1 \pm 1.2	0.6	0.314 \pm 0.001
3g	3.6 \pm 0.6	6.2 \pm 0.5	0.6	0.069 \pm 0.003
3h	21.8 \pm 6.4	19.3 \pm 2.8	1.1	0.070 \pm 0.006
3i	22.1 \pm 3.9	20.2 \pm 3.0	1.1	0.173 \pm 0.005
3j	44.3 \pm 3.8	23.6 \pm 4.8	1.9	0.074 \pm 0.004
3k	19.5 \pm 1.7	4.7 \pm 0.6	4.1	0.052 \pm 0.001
3l	27.9 \pm 5.0	11.7 \pm 4.6	2.4	0.044 \pm 0.007
3m	8.3 \pm 0.8	5.2 \pm 0.6	1.6	0.223 \pm 0.002
3n	4.4 \pm 1.0	5.6 \pm 0.7	0.8	0.081 \pm 0.004
3o	3.7 \pm 0.6	1.4 \pm 0.4	2.6	0.114 \pm 0.003
3p	4.8 \pm 0.8	2.0 \pm 0.8	2.4	0.012 \pm 0.007
3q	5.5 \pm 0.9	1.6 \pm 0.3	3.4	0.301 \pm 0.004
3r	10.1 \pm 0.7	1.0 \pm 0.3	10.1	0.102 \pm 0.004
3s	9.4 \pm 0.8	1.8 \pm 0.3	5.2	0.139 \pm 0.001
3t	10.8 \pm 1.0	1.9 \pm 1.8	5.7	0.193 \pm 0.003
3u	69.8 \pm 25.5	40.3 \pm 5.2	1.7	nd
4	12.7 \pm 1.9	26.3 \pm 5.7	0.5	nd
tacrine	69.8 \pm 11.1	10.6 \pm 1.1	6.6	0.001 \pm 0.001
ISDN	nd	nd	nd	0.382 \pm 0.003

^aData is the mean of at least three determinations. ^bSelectivity ratio = $(IC_{50}$ of AChE)/(IC_{50} of BuChE). ^cAll values are the mean \pm SEM. ^dnd means not determined.

Behavioral Studies. To gain more insight into the therapeutic potential of the hybrid compounds, behavioral studies were assayed using passive avoidance test.³⁶ Scopolamine-induced cognition impaired adult mice were used as the animal model to measure the cognitive improving effects of compounds **1b**, **3f**, and **3u** in comparison to tacrine. Measuring was performed in a step-through passive avoidance apparatus, which contained two symmetrical compartments, a dark and a light chamber. Mice were first placed in the light chamber, and they would spontaneously enter the dark chamber, however the entry would be punished by low intensity electric foot shocks (0.4 mA). After the mice were adapted to the apparatus, they were treated with tacrine (1.978 μ mol/100 g b wt) or test compounds **1b**, **3f**, and **3u** (equimolar dose), respectively. Fifty-

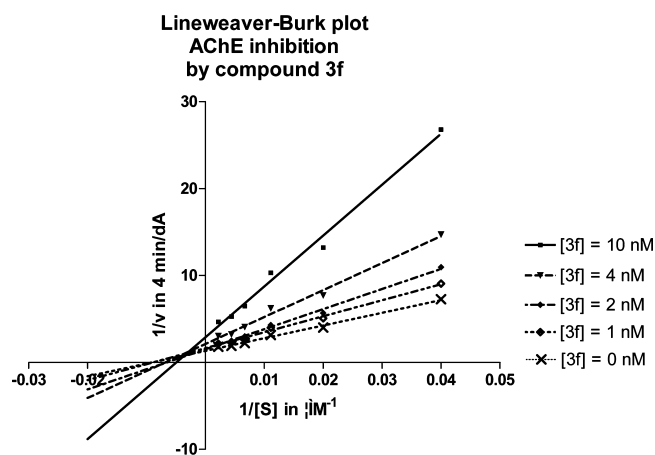


Figure 2. Lineweaver–Burk plots resulting from subvelocity curves of AChE activity with different substrate concentrations (25–450 μ M) in the absence and presence of 1, 2, 4, 10 nM **3f**.

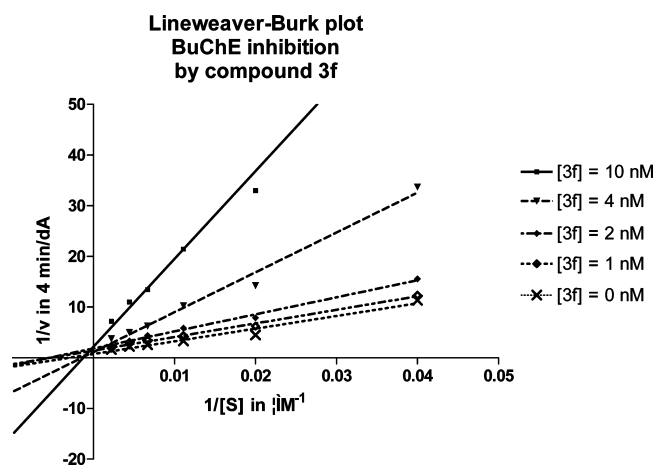


Figure 3. Lineweaver–Burk plots resulting from subvelocity curves of BuChE activity with different substrate concentrations (25–450 μ M) in the absence and presence of 1, 2, 4, 10 nM **3f**.

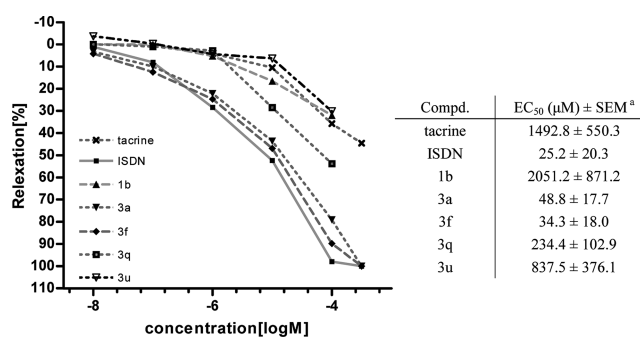


Figure 4. Concentration–response curves for the vasorelaxant effects of tacrine, ISDN, and compounds **1b**, **3a**, **3f**, **3q**, **3u**. ^aData are the mean values of at least three determinations.

five min later, scopolamine (0.2 mg/100 g b wt), which distinctly blocks the muscarinic cholinergic receptors, was administered to the animals. Then the first trial of 300 s for training started, and 24 h later, a second trial in which the shock was not delivered was carried out to test the retention. The number of errors made entering from the light room to the dark room in the first trial was recorded as the indication for short time learning ability (Figure 6). In addition, the other

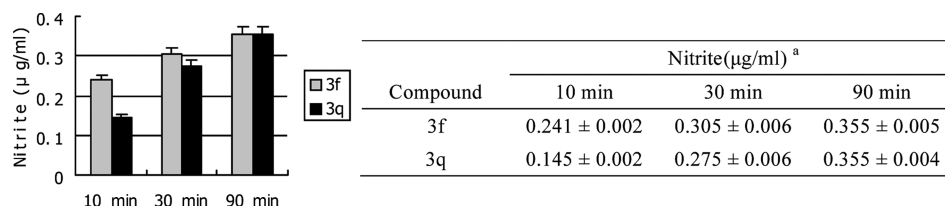


Figure 5. Variable levels of NO produced by 3f and 3q at 10, 30, and 90 min post-treatment. ^aAll values are the mean ± SEM. Determined by Griess reaction.

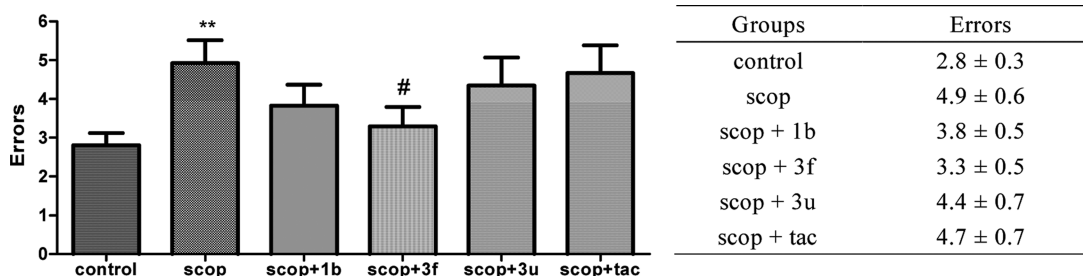


Figure 6. Effect of 1b, 3f, 3u, and tacrine (tac) on number of errors mice made entering from the light room to the dark room in the first trial. Values are expressed as mean ± SEM ($n = 8-9$, t test, $p^{**} \leq 0.01$ compared to the control group, $p^{\#} \leq 0.05$ compared to the scop group).

parameter, the transfer latency time (TLT in seconds) was taken to determine the cognitive improving potency of the test compounds (Figure 7).

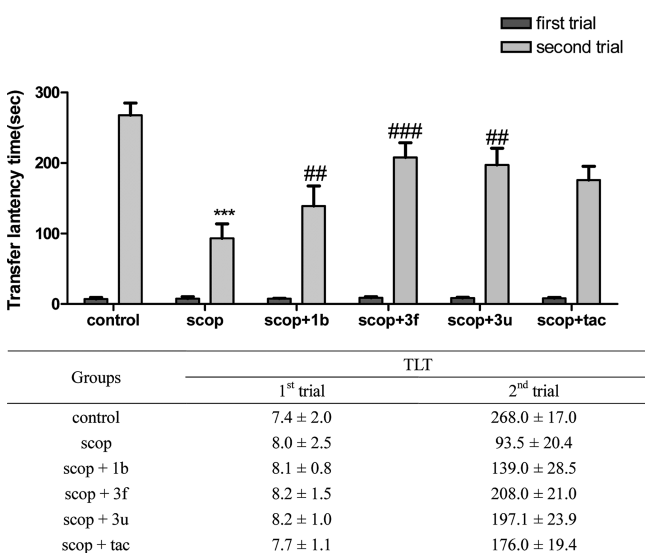


Figure 7. Effect of 1b, 3f, 3u, and tacrine (tac) on transfer latency time (TLT) in the PA test. Values are expressed as mean ± SEM ($n = 8-9$, t test, $p^{***} \leq 0.001$ compared to the control group, $p^{\#\#\#} \leq 0.01$, $p^{\#\#\#\#} \leq 0.001$ compared to the scop group).

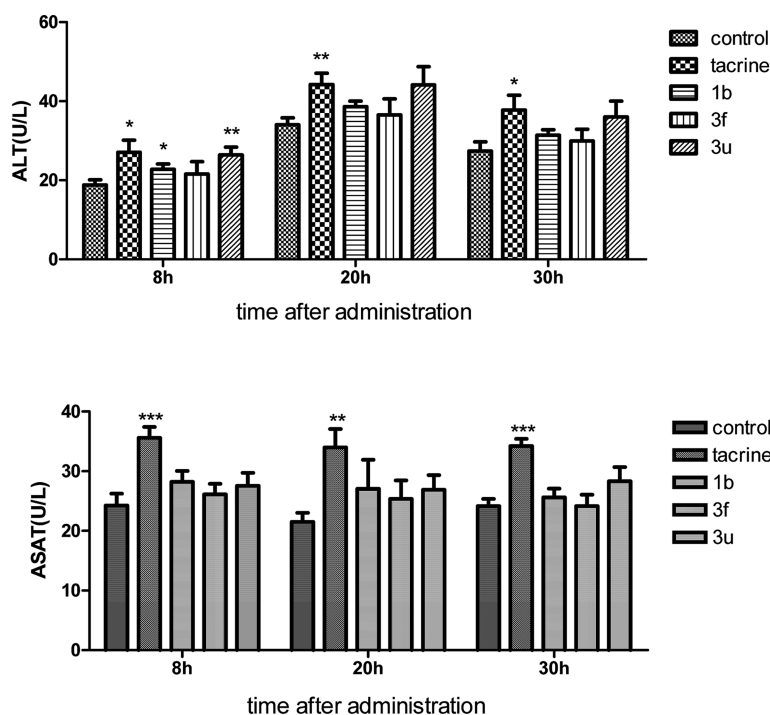
The results in Figure 6 showed that the error numbers of group treated with 1b, 3f, and 3u was lower than that of the scopolamine group, indicating the test compounds could benefit for short time learning ability. As for TLT (Figure 7), a significant increase in the 1b, 3f, and 3u group was observed in comparison to the scopolamine group, demonstrating that all the test compounds were active in improving memory impairment. As a consequence, 1b, 3f, and 3u all showed cognitive improving potency. 3f showed highest in vivo activity, compared with positive control tacrine and parent compound 1b. Furthermore, 3f possessed better performance than the

non-nitrate analogue 3u. These findings are consistent with the in vitro ChE inhibition activity and in vitro vasorelaxation effect, which illustrates again the importance of the nitrate group.

Hepatotoxicity Studies. The main disadvantage of tacrine is the high hepatotoxicity and it elevates levels of liver transaminase and decreases albumin concentration.³⁷ It has been reported that NO production in the liver is usually increased in response to acute insult with hepatotoxicants.³⁸ Moreover, some NO-donating drugs were found to exhibit hepatoprotective activity.^{28,31,39} To determine whether our nitrate containing test compounds can yield in decreased hepatotoxicity in comparison to tacrine and the non-nitrate parent compounds, 1b, 3f, and 3u were selected for the assay with adult mice. After being treated with tacrine, 1b, 3f, and 3u (equimolar doses), the heparinized serum of the mice was obtained after different times and the levels of aspartate aminotransferase (ASAT) and alanine aminotransferase (ALT) were determined (Figure 8). In comparison to the control, tacrine caused significant hepatotoxicity, as indicated by the increased activity of ASAT and ALT. 1b and 3f possessed higher safety than tacrine, and 3f showed the lowest hepatotoxicity among all the compounds.

For histological studies, liver tissues taken from the animals were stained with hematoxylin and eosin (HE). Paraffin sections were observed 30 h after administration of tacrine, 1b, 3f, and 3u. For the tacrine treated section, complete pericentral necrosis and distinct fatty degeneration of the hepatocytes of the surrounding intermediate and periportal zones could be seen (Figure 9B). Conversely, only minor morphological changes were observed after the treatment with test compounds (Figure 9C-E). All these findings give strong evidence that the introduction of nitrate group could improve the safety of the parent compound.

Molecular Modeling. A molecular modeling study using CDocker within Discovery Studio (DS, Accelrys) was performed to explore the binding mode of compound 1b, 3f, and 3u with the enzyme eeAChE. The crystal structure of the bis(7)-tacrine-AChE complex⁴⁰ was taken as a model because



Groups	ALT (U/L)			ASAT (U/L)		
	8h	20h	30h	8h	20h	30h
control	18.8 ± 1.3	34.1 ± 1.8	27.4 ± 2.3	24.3 ± 2.0	21.5 ± 1.5	23.8 ± 1.3
tacrine	27.1 ± 3.1	44.2 ± 2.8	37.8 ± 3.7	35.6 ± 1.9	34.0 ± 3.1	34.2 ± 1.2
1b	22.8 ± 1.3	38.6 ± 1.4	31.4 ± 1.4	28.2 ± 1.8	27.1 ± 4.8	25.6 ± 1.5
3f	21.6 ± 3.2	36.6 ± 4.1	30.0 ± 2.9	26.1 ± 1.8	25.4 ± 3.1	24.2 ± 1.9
3u	26.4 ± 1.9	44.1 ± 4.6	36.0 ± 4.0	27.6 ± 2.2	26.9 ± 2.5	28.3 ± 2.4

Figure 8. ALT and ASAT activity after the administration of tacrine, **1b**, **3f**, or **3u**. Values are expressed as mean ± SEM ($n = 8-9$, t test, compared to control of the same time after administration, $p^* \leq 0.05$, $p^{**} \leq 0.01$, $p^{***} \leq 0.001$).

of the similarity between the bis-tacrine and our compounds. A tacrine fragment and a long flexible side chain were contained in bis(7)-tacrine and our compounds. The proposed binding model of **1b**, **3f**, and **3u** with the key residues in the gorge site was shown in Figure 10. The superimposition of the three compounds with bis(7)-tacrine indicated that our compound can cover the binding gorge in a satisfactory orientation and conformation, thus leading to the high inhibitory potency. The binding model suggested the tacrine fragment of all of the three compounds was bound to near the bottom of the gorge in a similar arrangement. Tacrine fragment showed strong parallel $\pi-\pi$ stacking against the indole ring of Trp84 and the imidazole ring of His440 in all cases. In the middle of the gorge, the constricted region, the aliphatic alkyl chains of **1b**, **3f**, and **3u** were located as linkers and surrounded with phenyl rings of Tyr121, Phe330, and Tyr334. The $\pi-\pi$ stacking interaction between the tacrine fragment and the benzene ring of Phe330 was observed. The cyclohexane ring of tacrine may have van der Waals contact with Ser200 and Gly441 (distances between the closest carbon atoms of 3.9 and 4.0 Å). The binding modes of the three compounds and bis(7)-tacrine were found to be very similar, which might explain why these compounds exhibited very potent AChE inhibitory effects. At the mouth of the gorge, the benzene ring of ferulic acid group in compounds **1b**, **3f**, and **3u** showed the hydrophobic interaction with the residues Tyr70 (distance between the closest carbon

atoms was 3.7 Å, respectively), the key residue in PAS. It has been estimated that the PAS site was about 20 Å deep from the CAS.⁴¹ **3f** and **3u** had a length of 21.0 and 19.1 Å, respectively, which was enough to cover both the PAS and CAS, leading our compounds acting as “dual binding site” inhibitors. The NO-donating group in **3f** could form a hydrogen bond with Asp276, which stabilized the binding interaction with AChE, whereas in **3u** and **1b**, the corresponding interaction was missing due to the lack of NO-donating group. This finding could explain the higher potency of **3f** compared to **3u** and **1b**. The $-CDOCKER$ energies for **1b**, **3f**, and **3u** (37.23, 43.86, and 35.38, respectively) correlated well with their inhibitory effect. As a further test, we have calculated the relative binding affinity between the three compounds and AChE by means of MM/PBSA method. The results indicated that binding of **3f** to AChE was more favored by near 15.0 and 22.8 kcal/mol relative to **1b** and **3u**. Both the $-CDOCKER$ energy and MM/PBSA calculations confirmed the higher potency of **3f**.

CONCLUSIONS

A series of NO-donating tacrine-ferulic acid hybrid compounds have been designed and synthesized as novel multifunctional potent ChEs inhibitors. All of the compounds effectively inhibited ChEs in the nanomolar range in vitro. Compound **3f** was one of the most potent inhibitors that was 5-fold and 2-fold more active than the parent compound **1b**

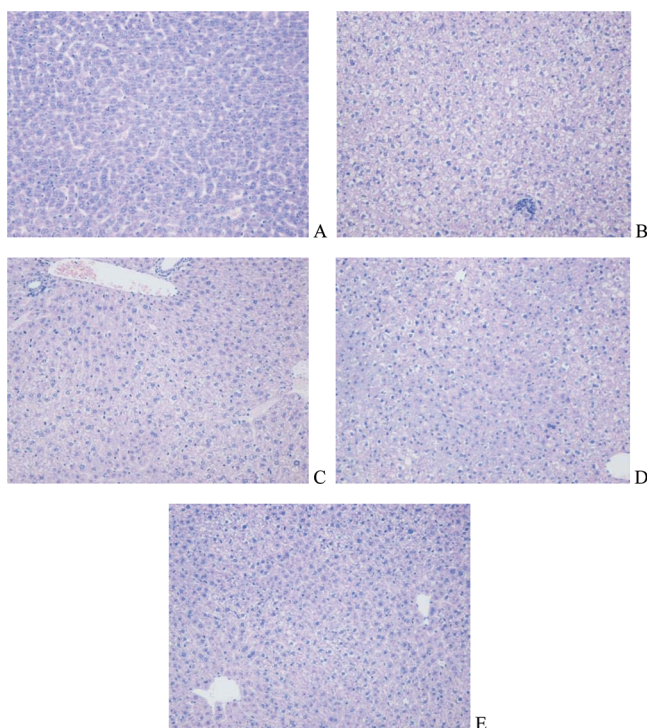


Figure 9. Histomorphological appearance of livers of male mice after treatment with the solvent only (control) (A) or 30 h after administration of tacrine (B), **1b** (C), **3f** (D), or **3u** (E). HE, original magnification $\times 200$.

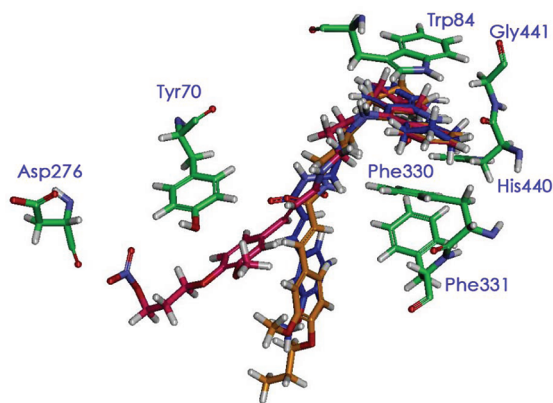


Figure 10. Representation of the binding mode of compound **3f** (purple), **1b** (blue), and **3u** (yellow) with AChE (PDB id: 2CKM). The key residues that interacted with the three molecules were colored in light green.

toward AChE and BuChE, respectively. In the vascular relaxation assay, **3f** possessed an activity, positively correlated with the NO production and comparable to the activity of the reference ISDN. Evaluated by the scopolamine-induced cognition impairment animal model, **3f** showed significant cognition improving activity. In addition, hepatotoxicity studies confirmed that **3f** was much safer than tacrine as well as **1b**. The priority of **3f** to **3u** (the analogue of **3f** without the nitrate group) in all the tests demonstrated that the strategy of NO-donating drugs was rational and beneficial. Altogether, the multifunctional effects of the new hybrids qualified them as potential anti-AD drug candidates and **3f** might be considered as a promising lead compound for further research.

EXPERIMENTAL SECTION

Chemistry. Melting points are uncorrected and were measured in open capillary tubes using a Gallenkamp melting point apparatus. ^1H and ^{13}C NMR spectral data were obtained from a Bruker Avance 250 spectrometer (250 MHz). Considering the series containing closely related compounds, the protons and carbons are assigned for instance in **3a**, **3u**, and **4**. HRMS data were recorded using Agilent technologies LC/MSD TOF. TLC was performed on silica gel F254 plates (Merck). Column chromatography was carried out with silica gel 60, 63–200 μm (Baker). Purities of the compounds were determined by elemental analysis performed on a Heraeus Vario EL III apparatus (Firma Elementar Analysensysteme GmbH, Germany). All values for C, H, and N were found to be within $\pm 0.4\%$ of the theoretical values. All compounds showed $>95\%$ purity.

(E)-Methyl 3-[4-(Bromoalkoxy)-3-methoxyphenyl]acrylates 6a–6d: General Procedure I. A mixture of **5** and 3 molar equiv of dibromoalkane in DMF (50 mL) was treated with a molar equiv of K_2CO_3 . After being stirred at 60°C for 6 h, the reaction mixture was cooled down to room temperature, poured into water, and extracted with ethyl acetate (3×15 mL). The combined organic layers were washed with brine, dried over anhydrous Na_2SO_4 , and evaporated under reduced pressure to give the crude product. The purification was performed by column chromatography (ethyl acetate/petrol ether = 1/4, v/v).

(E)-Methyl 3-[3-Methoxy-4-[(nitrooxy)alkoxy]phenyl]acrylates 7a–7d: General Procedure II. Compounds **6a–6d** and 1.2 molar equiv of AgNO_3 in 50 mL of CH_3CN were stirred at 60°C for 6 h under dark condition. Then the resulting mixture was cooled to room temperature and filtered to give a brown filtrate, which was evaporated under reduced pressure. The residue was purified by recrystallization from CH_3CN .

(E)-3-[3-Methoxy-4-[(nitrooxy)alkoxy]phenyl] Acrylic Acids 8a–8d: General Procedure III. Three molar equiv of $\text{LiOH}\cdot\text{H}_2\text{O}$ were added to a solution of compound **7** in a 15/5/5 mL mixture of THF/MeOH/ H_2O , and the mixture was stirred at room temperature for 24 h. After removing the solvent under reduced pressure, the residue was diluted with H_2O (30 mL), acidified to pH = 4 with 10% HCl, and extracted with ethyl acetate (3×15 mL). The combined organic layers were washed with brine, dried over anhydrous Na_2SO_4 , and evaporated in vacuo to give the crude product, which was recrystallized from ethyl acetate.

9-Aminoalkylamino-1,2,3,4-tetrahydroacridines 10a–10e: General Procedure IV. To a solution of **9** (9-Chlorotetrahydroacridine) in 10 mL of pentanol three molar equiv of diaminolkane were added. After refluxing for 18 h under nitrogen, the solution was cooled to 0°C and then acidified to pH = 2 with HCl/ether solution. The deposit was separated, dissolved in 10 mL of water, and then the solution was basified to pH = 10 with a saturated aqueous solution of Na_2CO_3 and extracted with CH_2Cl_2 (3×10 mL). The combined organic layers were washed with brine, dried over anhydrous Na_2SO_4 , and evaporated in vacuo. The residue was purified by column chromatography ($\text{CH}_2\text{Cl}_2/\text{MeOH} = 7/3$, v/v, plus 5 mL triethylamine per 1000 mL).

{2-Methoxy-4-[(1E)-3-oxo-3-((1,2,3,4-tetrahydroacridin-9-ylamino)alkylamino)prop-1-enyl]phenoxy}alkyl Nitrates 3a–3t: General Procedure V. Compound **8** and a molar equiv amount of N,N' -dicyclohexylcarbodiimide (DCC) were dissolved in 20 mL of dry CH_2Cl_2 , and the mixture was stirred at room temperature for 0.5 h. Then a solution of a molar equiv amount of **10** in 5 mL of dry CH_2Cl_2 was added, followed by a catalytic amount of 4-dimethylaminopyridine (DMAP). After being stirred for 24 h at room temperature, the reaction was quenched by adding 10 mL of H_2O . Then the resulting mixture was filtered, and the filtrate was extracted with CH_2Cl_2 (3×15 mL). The combined organic phases were washed with brine, dried over anhydrous Na_2SO_4 , and evaporated in vacuo. The residue was purified by column chromatography ($\text{CH}_2\text{Cl}_2/\text{MeOH} = 10/1$, v/v).

2-[2-Methoxy-4-[(1E)-3-oxo-3-(2-(1,2,3,4-tetrahydroacridin-9-ylamino)ethylamino)prop-1-enyl]phenoxy]ethyl Nitrate (3a). Following general procedure V, compound **10a** (0.24 g, 1 mmol) reacted with compound **8a** (0.28 g, 1 mmol) to furnish **3a** as a yellow

solid (0.15 g, 30%); mp 63–65 °C. ^1H NMR (CDCl_3): δ 8.00–7.87 (m, 2H, arom), 7.58 (d, $J = 15.5$ Hz, 1H, $\text{COCH}=\text{CH}$), 7.50–7.44 (t, 1H, arom), 7.30–7.24 (t, 1H, arom), 7.04–7.00 (m, 3H, arom, CONH), 6.82–6.79 (d, 1H, arom), 6.42 (d, $J = 15.5$ Hz, 1H, $\text{COCH}=\text{CH}$), 5.32 (br, 1H, NH), 4.83–4.80 (t, 2H, OCH_2), 4.30–4.26 (t, 2H, CH_2ONO_2), 3.82 (s, 3H, OCH_3), 3.73 (br, 4H, $\text{NHCH}_2\text{CH}_2\text{NHCO}$), 2.99 (br, 2H, $\text{C}4-\text{H}_2$), 2.66 (br, 2H, $\text{C}1-\text{H}_2$), 1.82 (br, 4H, $\text{C}2-\text{H}_2$, $\text{C}3-\text{H}_2$). ^{13}C NMR (CDCl_3): δ 167.69 (NHCO), 156.97 (arom), 151.49 (arom), 149.95 (arom), 149.02 (arom), 145.57 (arom), 141.05 ($\text{COCH}=\text{CH}$), 129.21 (arom), 128.97 (arom), 126.79 (arom), 123.92 (arom), 122.98 (arom), 121.60 (arom), 119.15 ($\text{COCH}=\text{CH}$), 118.93 (arom), 115.28 (arom), 114.34 (arom), 110.89 (arom), 70.89 (OCH_2), 65.54 (CH_2ONO_2), 55.95 (OCH_3), 50.02 (NHCH_2), 40.55 (CH_2NHCO), 32.84 ($\text{C}4$), 24.84 ($\text{C}1$), 22.81 ($\text{C}3$), 22.29 ($\text{C}2$). HRMS (ESI) m/z calcd for $\text{C}_{27}\text{H}_{30}\text{N}_4\text{O}_6$ [M^+] 506.2165; found 506.2170. Anal. Calcd for ($\text{C}_{27}\text{H}_{30}\text{N}_4\text{O}_6 \cdot \frac{3}{4}\text{H}_2\text{O}$): found C, 62.42; H, 6.17; N, 11.03; requires C, 62.36; H, 6.10; N, 10.77.

3-[2-Methoxy-4-[(1E)-3-oxo-3-(2-(1,2,3,4-tetrahydroacridin-9-ylamino)ethylamino)prop-1-enyl]phenoxy]propyl Nitrate (3b). Compound 10a (0.24 g, 1 mmol) reacted with compound 8b (0.30 g, 1 mmol) to furnish 3b as a yellow solid (0.18 g, 35%); mp 60–62 °C. ^1H NMR (CDCl_3): δ 7.97–7.83 (m, 2H), 7.57 (d, $J = 15.5$ Hz, 1H), 7.49–7.43 (t, 1H), 7.30–7.24 (t, 1H), 7.03–6.97 (m, 3H), 6.80–6.77 (d, 1H), 6.36 (d, $J = 15.5$ Hz, 1H), 5.07 (br, 1H), 4.69–4.64 (t, 2H), 4.11–4.07 (t, 2H), 3.80 (s, 3H), 3.68 (br, 4H), 2.97 (br, 2H), 2.66 (br, 2H), 2.27–2.18 (m, 2H), 1.81 (br, 4H). ^{13}C NMR (CDCl_3): δ 167.68, 157.81, 151.04, 149.63, 149.56, 146.45, 141.20, 128.63, 128.36, 127.62, 123.81, 122.82, 121.73, 119.60, 118.49, 115.73, 113.24, 110.50, 69.87, 64.84, 55.86, 49.91, 40.64, 33.37, 26.88, 24.97, 22.91, 22.49. HRMS (ESI) m/z calcd for $\text{C}_{28}\text{H}_{32}\text{N}_4\text{O}_6$ [M^+] 520.2322; found 520.2325. Anal. Calcd for ($\text{C}_{28}\text{H}_{32}\text{N}_4\text{O}_6 \cdot \text{H}_2\text{O}$): found C, 62.35; H, 6.33; N, 10.29; requires C, 62.44; H, 6.36; N, 10.40.

4-[2-Methoxy-4-[(1E)-3-oxo-3-(2-(1,2,3,4-tetrahydroacridin-9-ylamino)ethylamino)prop-1-enyl]phenoxy]butyl Nitrate (3c). Compound 10a (0.24 g, 1 mmol) reacted with compound 8c (0.31 g, 1 mmol) to furnish 3c as a yellow solid (0.19 g, 36%); mp 46–48 °C. ^1H NMR (CDCl_3): δ 7.97–7.84 (m, 2H), 7.57 (d, $J = 15.5$ Hz, 1H), 7.51–7.45 (t, 1H), 7.31–7.25 (t, 1H), 7.02–6.94 (m, 2H), 6.79–6.76 (d, 2H), 6.31 (d, $J = 15.5$ Hz, 1H), 4.85 (br, 1H), 4.56–4.51 (t, 2H), 4.03 (br, 2H), 3.79 (s, 3H), 3.66 (br, 4H), 2.99 (br, 2H), 2.68 (br, 2H), 1.93 (br, 4H), 1.82 (br, 4H). ^{13}C NMR (CDCl_3): δ 167.58, 158.42, 150.66, 149.89, 149.52, 147.11, 141.33, 128.39, 128.30, 127.91, 123.77, 122.66, 121.85, 119.93, 118.20, 116.13, 112.69, 110.27, 72.92, 68.13, 55.83, 49.84, 40.72, 33.82, 25.34, 25.06, 23.89, 23.00, 22.65. HRMS (ESI) m/z calcd for $\text{C}_{29}\text{H}_{34}\text{N}_4\text{O}_6$ [M^+] 534.2478; found 534.2483. Anal. Calcd for ($\text{C}_{29}\text{H}_{34}\text{N}_4\text{O}_6 \cdot \frac{3}{4}\text{H}_2\text{O}$): found C, 63.68; H, 6.33; N, 10.14; requires C, 63.55; H, 6.53; N, 10.22.

6-[2-Methoxy-4-[(1E)-3-oxo-3-(2-(1,2,3,4-tetrahydroacridin-9-ylamino)ethylamino)prop-1-enyl]phenoxy]hexyl Nitrate (10d). Compound 10a (0.24 g, 1 mmol) reacted with compound 8d (0.34 g, 1 mmol) to furnish 3d as a yellow solid (0.16 g, 28%); mp 50–52 °C. ^1H NMR (CDCl_3): δ 7.97–7.85 (m, 2H), 7.57 (d, $J = 15.5$ Hz, 1H), 7.52–7.46 (t, 1H), 7.32–7.26 (t, 1H), 7.04–6.97 (m, 2H), 6.82–6.79 (d, 1H), 6.56 (br, 1H), 6.29 (d, $J = 15.5$ Hz, 1H), 4.84 (br, 1H), 4.47–4.41 (t, 2H), 4.04–3.99 (t, 2H), 3.82 (s, 3H), 3.67 (br, 4H), 3.00 (br, 2H), 2.69 (br, 2H), 1.84–1.69 (m, 8H), 1.50–1.47 (m, 4H). ^{13}C NMR (CDCl_3): δ 167.57, 158.36, 150.66, 150.23, 149.46, 147.05, 141.473, 128.41, 128.31, 127.57, 123.79, 122.64, 121.98, 119.92, 117.96, 116.14, 112.51, 110.26, 73.20, 68.64, 55.93, 49.82, 40.72, 33.79, 28.81, 26.65, 25.58, 25.42, 25.05, 23.00, 22.65. HRMS (ESI) m/z calcd for $\text{C}_{31}\text{H}_{38}\text{N}_4\text{O}_6$ [M^+] 562.2791; found 562.2796. Anal. Calcd for ($\text{C}_{31}\text{H}_{38}\text{N}_4\text{O}_6 \cdot \frac{3}{4}\text{H}_2\text{O}$): found C, 64.52; H, 6.93; N, 9.47; requires C, 64.62; H, 6.90; N, 9.72.

2-[2-Methoxy-4-[(1E)-3-oxo-3-(1,2,3,4-tetrahydroacridin-9-ylamino)propylamino]prop-1-enyl]phenoxy]ethyl Nitrate (3e). Compound 10b (0.26 g, 1 mmol) reacted with compound 8a (0.28 g, 1 mmol) to furnish 3e as a yellow solid (0.18 g, 35%); mp 59–61 °C. ^1H NMR (CDCl_3): δ 8.05–7.88 (m, 2H), 7.57 (d, $J = 15.5$

Hz, 1H), 7.53–7.49 (t, 1H), 7.35–7.31 (t, 1H), 7.01–6.98 (m, 2H), 6.81–6.79 (d, 1H), 6.74–6.71 (t, 1H), 6.37 (d, $J = 15.5$ Hz, 1H), 5.02 (br, 1H), 4.81–4.79 (t, 2H), 4.28–4.26 (t, 2H), 3.80 (s, 3H), 3.55–3.51 (m, 4H), 3.03 (br, 2H), 2.75 (br, 2H), 1.87–1.83 (m, 6H). ^{13}C NMR (CDCl_3): δ 166.98, 158.04, 150.94, 150.03, 148.95, 146.68, 140.59, 129.47, 128.56, 127.85, 123.88, 122.76, 121.46, 120.08, 119.36, 116.11, 114.61, 110.06, 70.94, 65.67, 55.94, 45.36, 36.83, 33.51, 31.53, 25.07, 22.99, 22.59. HRMS (ESI) m/z calcd for $\text{C}_{28}\text{H}_{32}\text{N}_4\text{O}_6$ [M^+] 520.2322; found 520.2325. Anal. Calcd for ($\text{C}_{28}\text{H}_{32}\text{N}_4\text{O}_6 \cdot \text{H}_2\text{O}$): found C, 62.57; H, 6.33; N, 10.23; requires C, 62.44; H, 6.36; N, 10.40.

3-[2-Methoxy-4-[(1E)-3-oxo-3-(1,2,3,4-tetrahydroacridin-9-ylamino)propylamino]prop-1-enyl]phenoxy]propyl Nitrate (3f). Compound 10b (0.26 g, 1 mmol) reacted with compound 8b (0.30 g, 1 mmol) to furnish 3f as a yellow solid (0.17 g, 32%); mp 53–55 °C. ^1H NMR (CDCl_3): δ 8.06–7.89 (m, 2H), 7.59 (d, $J = 15.5$ Hz, 1H), 7.55–7.51 (t, 1H), 7.36–7.33 (t, 1H), 7.05–6.99 (m, 2H), 6.83–6.81 (d, 1H), 6.47–6.44 (t, 1H), 6.34 (d, $J = 15.5$ Hz, 1H), 4.99 (br, 1H), 4.70–4.67 (t, 2H), 4.13–4.10 (t, 2H), 3.83 (s, 3H), 3.56–3.51 (m, 4H), 3.05 (br, 2H), 2.77 (br, 2H), 2.27–2.21 (m, 2H), 1.90–1.82 (m, 6H). ^{13}C NMR (CDCl_3): δ 166.98, 158.19, 150.82, 149.78, 149.58, 146.86, 140.91, 128.60, 128.49, 128.11, 123.88, 122.70, 121.67, 120.18, 118.80, 116.26, 113.53, 110.66, 69.89, 64.99, 55.90, 45.41, 36.88, 33.65, 31.58, 26.98, 25.10, 23.04, 22.66. HRMS (ESI) m/z calcd for $\text{C}_{29}\text{H}_{34}\text{N}_4\text{O}_6$ [M^+] 534.2478; found 534.2480. Anal. Calcd for ($\text{C}_{29}\text{H}_{34}\text{N}_4\text{O}_6 \cdot \frac{3}{4}\text{H}_2\text{O}$): found C, 63.72; H, 6.50; N, 10.22; requires C, 63.55; H, 6.53; N, 10.22.

4-[2-Methoxy-4-[(1E)-3-oxo-3-(1,2,3,4-tetrahydroacridin-9-ylamino)propylamino]prop-1-enyl]phenoxy]butyl Nitrate (3g). Compound 10b (0.26 g, 1 mmol) reacted with compound 8c (0.31 g, 1 mmol) to furnish 3g as a yellow solid (0.18 g, 33%); mp 50–52 °C. ^1H NMR (CDCl_3): δ 8.06–7.88 (m, 2H), 7.62–7.49 (m, 2H), 7.37–7.31 (t, 1H), 7.05–6.97 (m, 2H), 6.82–6.78 (d, 1H), 6.38–6.28 (m, 2H), 4.95 (br, 1H), 4.57–4.53 (t, 2H), 4.07–4.03 (t, 2H), 3.82 (s, 3H), 3.54–3.51 (m, 4H), 3.04 (br, 2H), 2.76 (br, 2H), 1.96–1.80 (m, 10H). ^{13}C NMR (CDCl_3): δ 167.00, 158.35, 150.67, 149.82, 149.53, 147.03, 141.06, 128.40, 128.29, 128.03, 123.84, 122.66, 121.82, 120.25, 118.41, 116.36, 112.72, 110.24, 72.91, 68.14, 55.84, 45.35, 36.84, 33.80, 31.57, 25.35, 25.13, 23.91, 23.05, 22.71. HRMS (ESI) m/z calcd for $\text{C}_{30}\text{H}_{36}\text{N}_4\text{O}_6$ [M^+] 548.2635; found 548.2639. Anal. Calcd for ($\text{C}_{30}\text{H}_{36}\text{N}_4\text{O}_6 \cdot \frac{3}{4}\text{H}_2\text{O}$): found C, 63.96; H, 6.63; N, 9.67; requires C, 64.10; H, 6.72; N, 9.97.

6-[2-Methoxy-4-[(1E)-3-oxo-3-(1,2,3,4-tetrahydroacridin-9-ylamino)propylamino]prop-1-enyl]phenoxy]hexyl Nitrate (3h). Compound 10b (0.26 g, 1 mmol) reacted with compound 8d (0.34 g, 1 mmol) to furnish 3h as a yellow solid (0.18 g, 31%); mp 54–56 °C. ^1H NMR (CDCl_3): δ 8.05–7.86 (m, 2H), 7.62–7.48 (m, 2H), 7.36–7.30 (t, 1H), 7.03–6.96 (m, 2H), 6.81–6.78 (d, 1H), 6.54–6.49 (t, 1H), 6.32 (d, $J = 15.5$ Hz, 1H), 4.92 (br, 1H), 4.46–4.41 (t, 2H), 4.03–3.98 (t, 2H), 3.80 (s, 3H), 3.53–3.51 (m, 4H), 3.02 (br, 2H), 2.75 (br, 2H), 1.87–1.71 (m, 10H), 1.49–1.48 (m, 4H). ^{13}C NMR (CDCl_3): δ 167.07, 158.45, 150.61, 150.11, 149.44, 147.17, 141.04, 128.38, 128.33, 127.71, 123.79, 122.66, 121.66, 120.31, 118.30, 116.39, 112.53, 110.23, 73.20, 68.63, 55.90, 49.00, 45.35, 36.81, 31.88, 31.57, 28.82, 26.64, 25.57, 25.42, 23.06, 22.73. HRMS (ESI) m/z calcd for $\text{C}_{32}\text{H}_{40}\text{N}_4\text{O}_6$ [M^+] 576.2948; found 576.2955. Anal. Calcd for ($\text{C}_{32}\text{H}_{40}\text{N}_4\text{O}_6 \cdot \frac{1}{2}\text{H}_2\text{O}$): found C, 65.60; H, 7.27; N, 9.37; requires C, 65.62; H, 7.06; N, 9.57.

2-[2-Methoxy-4-[(1E)-3-oxo-3-(1,2,3,4-tetrahydroacridin-9-ylamino)butylamino]prop-1-enyl]phenoxy]ethyl Nitrate (3i). Compound 10c (0.27 g, 1 mmol) reacted with compound 8a (0.28 g, 1 mmol) to furnish 3i as a yellow solid (0.17 g, 32%); mp 45–47 °C. ^1H NMR (CDCl_3): δ 7.94–7.88 (m, 2H), 7.56–7.50 (m, 2H), 7.36–7.30 (t, 1H), 7.02–6.98 (m, 2H), 6.83–6.80 (d, 1H), 6.27 (d, $J = 15.5$ Hz, 1H), 6.11 (br, 1H), 4.84–4.80 (t, 2H), 4.30–4.27 (t, 2H), 4.03 (br, 1H), 3.82 (s, 3H), 3.51–3.49 (m, 2H), 3.45–3.40 (m, 2H), 3.03 (br, 2H), 2.68 (br, 2H), 1.88 (br, 4H), 1.69 (br, 4H). ^{13}C NMR (CDCl_3): δ 166.13, 158.40, 150.57, 149.93, 148.85, 147.20, 140.46, 129.42, 128.49, 128.42, 123.80, 122.71, 121.47, 120.21, 119.34, 116.22, 114.39, 110.78, 70.89, 65.55, 55.92, 48.87, 39.27, 33.87, 28.99, 26.64, 27.22, 24.82, 22.97, 22.70. HRMS (ESI) m/z calcd for $\text{C}_{29}\text{H}_{34}\text{N}_4\text{O}_6$

[M^+] 534.2478; found 534.2483. Anal. Calcd for ($C_{29}H_{34}N_4O_6 \cdot 3/4 H_2O$): found C, 63.38; H, 6.51; N, 10.31; requires C, 63.55; H, 6.53; N, 10.22.

3-[2-Methoxy-4-[(1E)-3-oxo-3-(4-(1,2,3,4-tetrahydroacridin-9-ylamino)butylamino)prop-1-enyl]phenoxy]propyl Nitrate (3j). Compound **10c** (0.27 g, 1 mmol) reacted with compound **8b** (0.30 g, 1 mmol) to furnish **3j** as a yellow solid (0.17 g, 31%); mp 40–42 °C. 1H NMR ($CDCl_3$): δ 7.95–7.88 (m, 2H), 7.57–7.50 (m, 2H), 7.35–7.29 (t, 1H), 7.02–6.97 (m, 2H), 6.82–6.79 (d, 1H), 6.29 (d, $J = 15.5$ Hz, 1H), 6.23–6.19 (t, 1H), 4.70–4.65 (t, 2H), 4.12–4.08 (t, 3H), 3.81 (s, 3H), 3.52–3.47 (m, 2H), 3.44–3.37 (m, 2H), 3.03 (br, 2H), 2.67 (br, 2H), 2.28–2.18 (m, 2H), 1.88–1.86 (m, 4H), 1.68 (br, 4H). ^{13}C NMR ($CDCl_3$): δ 166.27, 158.18, 150.73, 149.64, 149.40, 146.94, 140.58, 128.59, 128.51, 128.21, 123.82, 122.77, 121.62, 120.07, 118.98, 116.03, 113.31, 110.42, 69.88, 64.87, 55.86, 48.84, 39.23, 33.69, 28.96, 27.20, 26.90, 24.78, 22.94, 22.61. HRMS (ESI) m/z calcd for $C_{30}H_{36}N_4O_6 [M^+]$ 548.2635; found 548.2641. Anal. Calcd for ($C_{30}H_{36}N_4O_6 \cdot 1/2 H_2O$): found C, 64.30; H, 6.57; N, 9.85; requires C, 64.62; H, 6.69; N, 10.05.

4-[2-Methoxy-4-[(1E)-3-oxo-3-(4-(1,2,3,4-tetrahydroacridin-9-ylamino)butylamino)prop-1-enyl]phenoxy]butyl Nitrate (3k). Compound **10c** (0.27 g, 1 mmol) reacted with compound **8c** (0.31 g, 1 mmol) to furnish **3k** as a yellow solid (0.16 g, 28%); mp 39–41 °C. 1H NMR ($CDCl_3$): δ 7.94–7.87 (m, 2H), 7.57–7.49 (m, 2H), 7.35–7.29 (t, 1H), 7.01–6.96 (m, 2H), 6.80–6.76 (d, 1H), 6.27 (d, $J = 15.5$ Hz, 1H), 6.21–6.18 (t, 1H), 4.54 (br, 2H), 4.03 (br, 3H), 3.80 (s, 3H), 3.48–3.39 (m, 4H), 3.02 (br, 2H), 2.67 (br, 2H), 1.93–1.87 (m, 8H), 1.68 (br, 4H). ^{13}C NMR ($CDCl_3$): δ 166.30, 158.37, 150.58, 149.71, 149.51, 147.19, 140.66, 128.44, 128.40, 128.14, 123.77, 122.73, 121.74, 120.19, 118.73, 116.17, 112.72, 110.18, 72.92, 68.13, 55.82, 48.86, 39.24, 33.85, 28.98, 27.22, 25.34, 24.81, 23.89, 22.96, 22.67. HRMS (ESI) m/z calcd for $C_{31}H_{38}N_4O_6 [M^+]$ 562.2791; found 562.2798. Anal. Calcd for ($C_{31}H_{38}N_4O_6 \cdot 1/2 H_2O$): found C, 64.84; H, 6.98; N, 9.59; requires C, 65.13; H, 6.88; N, 9.80.

6-[2-Methoxy-4-[(1E)-3-oxo-3-(4-(1,2,3,4-tetrahydroacridin-9-ylamino)butylamino)prop-1-enyl]phenoxy]hexyl Nitrate (3l). Compound **10c** (0.27 g, 1 mmol) reacted with compound **8d** (0.34 g, 1 mmol) to furnish **3l** as a yellow solid (0.19 g, 32%); mp 43–45 °C. 1H NMR ($CDCl_3$): δ 7.94–7.87 (m, 2H), 7.57–7.49 (m, 2H), 7.35–7.29 (t, 1H), 7.03–6.97 (m, 2H), 6.81–6.78 (d, 1H), 6.26 (d, $J = 15.5$ Hz, 1H), 6.18–6.13 (t, 1H), 4.46–4.41 (t, 2H), 4.03–3.98 (t, 3H), 3.82 (s, 3H), 3.49 (br, 2H), 3.44–3.36 (m, 2H), 3.03 (br, 2H), 2.67 (br, 2H), 1.89–1.86 (m, 6H), 1.81–1.68 (m, 6H), 1.49–1.45 (m, 4H). ^{13}C NMR ($CDCl_3$): δ 166.35, 158.41, 150.58, 150.04, 149.43, 147.22, 140.76, 128.49, 128.39, 127.79, 123.78, 122.72, 121.85, 120.22, 118.51, 116.20, 112.52, 110.17, 73.20, 68.63, 55.91, 48.88, 39.25, 33.87, 28.99, 28.82, 27.23, 26.64, 25.57, 25.42, 24.81, 22.97, 22.68. HRMS (ESI) m/z calcd for $C_{33}H_{42}N_4O_6 [M^+]$ 590.3104; found 590.3112. Anal. Calcd for ($C_{33}H_{42}N_4O_6 \cdot 1/2 H_2O$): found C, 66.07; H, 7.20; N, 9.26; requires C, 66.09; H, 7.23; N, 9.34.

2-[2-Methoxy-4-[(1E)-3-oxo-3-(6-(1,2,3,4-tetrahydroacridin-9-ylamino)hexylamino)prop-1-enyl]phenoxy]ethyl Nitrate (3m). Compound **10d** (0.30 g, 1 mmol) reacted with compound **8a** (0.28 g, 1 mmol) to furnish **3m** as a yellow solid (0.20 g, 36%); mp 50–52 °C. 1H NMR ($CDCl_3$): δ 7.97–7.89 (m, 2H), 7.56–7.50 (m, 2H), 7.36–7.30 (t, 1H), 7.03–7.00 (m, 2H), 6.84–6.81 (d, 1H), 6.29 (d, $J = 15.5$ Hz, 1H), 5.94–5.90 (t, 1H), 4.84–4.80 (t, 2H), 4.31–4.27 (t, 2H), 4.03 (br, 1H), 3.83 (s, 3H), 3.50–3.45 (m, 2H), 3.40–3.32 (m, 2H), 3.05 (br, 2H), 2.69 (br, 2H), 1.91–1.89 (m, 4H), 1.68–1.62 (m, 2H), 1.58–1.50 (m, 2H), 1.41–1.39 (m, 4H). ^{13}C NMR ($CDCl_3$): δ 166.00, 158.25, 150.85, 149.95, 148.80, 147.17, 140.30, 129.51, 128.41, 123.66, 122.85, 121.42, 120.09, 119.51, 115.79, 114.44, 110.80, 70.90, 65.58, 55.92, 49.24, 39.47, 33.84, 31.58, 29.62, 26.58, 26.51, 24.77, 23.00, 22.70. HRMS (ESI) m/z calcd for $C_{31}H_{38}N_4O_6 [M^+]$ 562.2791; found 562.2799. Anal. Calcd for ($C_{31}H_{38}N_4O_6 \cdot 3/4 H_2O$): found C, 64.33; H, 6.90; N, 9.44; requires C, 64.62; H, 6.91; N, 9.72.

3-[2-Methoxy-4-[(1E)-3-oxo-3-(6-(1,2,3,4-tetrahydroacridin-9-ylamino)hexylamino)prop-1-enyl]phenoxy]propyl Nitrate (3n). Compound **10d** (0.30 g, 1 mmol) reacted with compound **8b** (0.30 g, 1 mmol) to furnish **3n** as a yellow solid (0.19 g, 33%); mp

45–47 °C. 1H NMR ($CDCl_3$): δ 7.96–7.88 (m, 2H), 7.56–7.50 (m, 2H), 7.36–7.30 (t, 1H), 7.03–6.98 (m, 2H), 6.82–6.79 (d, 1H), 6.29 (d, $J = 15.5$ Hz, 1H), 6.00–5.96 (t, 1H), 4.70–4.65 (t, 2H), 4.13–4.08 (t, 2H), 4.01 (br, 1H), 3.82 (s, 3H), 3.47 (br, 2H), 3.39–3.31 (m, 2H), 3.04 (br, 2H), 2.69 (br, 2H), 2.28–2.18 (m, 2H), 1.90 (br, 4H), 1.67–1.61 (m, 2H), 1.57–1.52 (m, 2H), 1.40–1.39 (m, 4H). ^{13}C NMR ($CDCl_3$): δ 166.11, 158.32, 150.81, 149.64, 149.35, 147.25, 140.44, 128.66, 128.49, 128.36, 123.64, 122.84, 121.57, 120.14, 119.10, 115.84, 113.33, 110.43, 69.89, 64.87, 55.85, 49.26, 39.46, 33.88, 31.59, 29.63, 26.91, 26.59, 26.52, 24.78, 23.01, 22.72. HRMS (ESI) m/z calcd for $C_{32}H_{40}N_4O_6 [M^+]$ 576.2948; found 576.2953. Anal. Calcd for ($C_{32}H_{40}N_4O_6 \cdot 3/4 H_2O$): found C, 65.22; H, 6.69; N, 9.09; requires C, 65.12; H, 7.09; N, 9.49.

4-[2-Methoxy-4-[(1E)-3-oxo-3-(6-(1,2,3,4-tetrahydroacridin-9-ylamino)hexylamino)prop-1-enyl]phenoxy]butyl Nitrate (3o). Compound **10d** (0.30 g, 1 mmol) reacted with compound **8c** (0.31 g, 1 mmol) to furnish **3o** as a yellow solid (0.19 g, 32%); mp 37–39 °C. 1H NMR ($CDCl_3$): δ 7.96–7.88 (m, 2H), 7.56–7.50 (m, 2H), 7.35–7.29 (t, 1H), 7.02–6.98 (m, 2H), 6.80–6.77 (d, 1H), 6.28 (d, $J = 15.5$ Hz, 1H), 6.01–5.97 (t, 1H), 4.54 (br, 2H), 4.04 (br, 3H), 3.81 (s, 3H), 3.46 (br, 2H), 3.39–3.31 (m, 2H), 3.04 (br, 2H), 2.68 (br, 2H), 1.93–1.89 (m, 8H), 1.66–1.61 (m, 2H), 1.57–1.52 (m, 2H), 1.39–1.38 (m, 4H). ^{13}C NMR ($CDCl_3$): δ 166.17, 158.36, 150.78, 149.66, 149.51, 147.31, 140.53, 128.52, 128.33, 128.21, 123.63, 122.83, 121.70, 120.16, 118.86, 115.86, 112.74, 110.20, 72.92, 68.14, 55.83, 49.26, 39.46, 33.91, 31.59, 29.63, 26.60, 26.53, 25.35, 24.79, 23.90, 23.01, 22.73. HRMS (ESI) m/z calcd for $C_{33}H_{42}N_4O_6 [M^+]$ 590.3104; found 590.3108. Anal. Calcd for ($C_{33}H_{42}N_4O_6 \cdot 3/4 H_2O$): found C, 65.47; H, 7.30; N, 9.14; requires C, 65.60; H, 7.26; N, 9.27.

6-[2-Methoxy-4-[(1E)-3-oxo-3-(6-(1,2,3,4-tetrahydroacridin-9-ylamino)hexylamino)prop-1-enyl]phenoxy]hexyl Nitrate (3p). Compound **10d** (0.30 g, 1 mmol) reacted with compound **8d** (0.34 g, 1 mmol) to furnish **3p** as a yellow solid (0.19 g, 31%); mp 38–40 °C. 1H NMR ($CDCl_3$): δ 7.96–7.88 (m, 2H), 7.56–7.50 (m, 2H), 7.35–7.30 (t, 1H), 7.02–6.98 (m, 2H), 6.82–6.78 (d, 1H), 6.28 (d, $J = 15.5$ Hz, 1H), 5.97–5.93 (t, 1H), 4.46–4.41 (t, 2H), 4.03–3.98 (t, 3H), 3.83 (s, 3H), 3.49–3.44 (t, 2H), 3.39–3.31 (m, 2H), 3.05 (br, 2H), 2.69 (br, 2H), 1.90–1.81 (m, 6H), 1.76–1.71 (m, 2H), 1.67–1.61 (m, 2H), 1.57–1.47 (m, 6H), 1.40–1.38 (m, 4H). ^{13}C NMR ($CDCl_3$): δ 166.20, 158.29, 150.82, 149.98, 149.44, 147.23, 140.61, 128.47, 128.36, 127.87, 123.64, 122.84, 121.80, 120.12, 118.67, 115.81, 112.54, 110.18, 73.20, 68.63, 55.91, 49.25, 39.45, 33.88, 31.58, 29.64, 28.83, 26.65, 26.59, 26.52, 25.57, 25.42, 24.78, 23.00, 22.72. HRMS (ESI) m/z calcd for $C_{35}H_{46}N_4O_6 [M^+]$ 618.3417; found 618.3423. Anal. Calcd for ($C_{35}H_{46}N_4O_6 \cdot 1/4 H_2O$): found C, 67.30; H, 7.69; N, 9.03; requires C, 67.45; H, 7.52; N, 8.99.

2-[2-Methoxy-4-[(1E)-3-oxo-3-(8-(1,2,3,4-tetrahydroacridin-9-ylamino)octylamino)prop-1-enyl]phenoxy]ethyl Nitrate (3q). Compound **10e** (0.31 g, 1 mmol) reacted with compound **3a** (0.28 g, 1 mmol) to furnish **3q** as a yellow solid (0.18 g, 31%); mp 40–42 °C. 1H NMR ($CDCl_3$): δ 7.97–7.89 (m, 2H), 7.56–7.50 (m, 2H), 7.36–7.30 (t, 1H), 7.02–6.99 (m, 2H), 6.82–6.79 (d, 1H), 6.33 (d, $J = 15.5$ Hz, 1H), 6.10–6.06 (t, 1H), 4.82–4.79 (t, 2H), 4.29–4.26 (t, 2H), 4.00 (br, 1H), 3.82 (s, 3H), 3.50–3.45 (t, 2H), 3.38–3.30 (m, 2H), 3.05 (br, 2H), 2.69 (br, 2H), 1.89 (br, 4H), 1.66–1.61 (m, 2H), 1.58–1.48 (m, 2H), 1.28 (br, 8H). ^{13}C NMR ($CDCl_3$): δ 166.00, 158.25, 150.96, 149.92, 148.74, 147.21, 140.13, 129.56, 128.39, 123.60, 122.92, 121.39, 120.06, 119.67, 115.66, 114.42, 110.78, 70.92, 65.56, 55.89, 49.35, 39.65, 33.85, 31.69, 29.60, 29.09, 26.73, 24.74, 23.00, 22.72. HRMS (ESI) m/z calcd for $C_{33}H_{42}N_4O_6 [M^+]$ 590.3104; found 590.3110. Anal. Calcd for ($C_{33}H_{42}N_4O_6 \cdot 1/2 H_2O$): found C, 65.99; H, 7.33; N, 9.24; requires C, 66.09; H, 7.23; N, 9.34.

3-[2-Methoxy-4-[(1E)-3-oxo-3-(8-(1,2,3,4-tetrahydroacridin-9-ylamino)octylamino)prop-1-enyl]phenoxy]propyl Nitrate (3r). Compound **10e** (0.31 g, 1 mmol) reacted with compound **3b** (0.30 g, 1 mmol) to furnish **3r** as a yellow solid (0.19 g, 31%); mp 39–41 °C. 1H NMR ($CDCl_3$): δ 7.99–7.93 (m, 2H), 7.58–7.51 (m, 2H), 7.38–7.32 (t, 1H), 7.06–7.02 (m, 2H), 6.85–6.82 (d, 1H), 6.32 (d, $J = 15.5$ Hz, 1H), 5.86–5.82 (t, 1H), 4.71–4.66 (t, 2H), 4.15–4.10 (t, 3H), 3.85 (s, 3H), 3.55–3.50 (t, 2H), 3.39–3.31 (m, 2H), 3.08 (br,

2H), 2.70 (br, 2H), 2.30–2.20 (m, 2H), 1.91 (br, 4H), 1.69–1.61 (m, 2H), 1.52–1.49 (m, 2H), 1.31 (br, 8H). ^{13}C NMR (CDCl_3): δ 166.03, 157.76, 151.31, 149.67, 149.34, 146.62, 140.39, 128.71, 127.94, 123.73, 122.98, 121.57, 119.77, 119.17, 115.33, 113.35, 110.41, 69.88, 64.88, 55.87, 49.31, 39.64, 33.45, 31.64, 29.62, 29.05, 26.93, 26.70, 24.65, 22.93, 22.58. HRMS (ESI) m/z calcd for $\text{C}_{34}\text{H}_{44}\text{N}_4\text{O}_6$ [M^+] 604.3261; found 604.3264. Anal. Calcd for ($\text{C}_{34}\text{H}_{44}\text{N}_4\text{O}_6$): found C, 67.29; H, 7.73; N, 8.89; requires C, 67.53; H, 7.33; N, 9.26.

4-{2-Methoxy-4-[(1E)-3-oxo-3-(8-(1,2,3,4-tetrahydroacridin-9-ylamino)octylamino)prop-1-enyl]phenoxy}butyl Nitrate (3s). Compound **10e** (0.31 g, 1 mmol) reacted with compound **8c** (0.31 g, 1 mmol) to furnish **3s** as a yellow solid (0.19 g, 31%); mp 35–37 °C. ^1H NMR (CDCl_3): δ 7.97–7.88 (m, 2H), 7.56–7.50 (m, 2H), 7.35–7.29 (t, 1H), 7.02–6.98 (m, 2H), 6.79–6.76 (d, 1H), 6.32 (d, $J = 15.5$ Hz, 1H), 6.13–6.08 (t, 1H), 4.56–4.51 (t, 2H), 4.03 (br, 3H), 3.80 (s, 3H), 3.50–3.44 (t, 2H), 3.38–3.30 (m, 2H), 3.04 (br, 2H), 2.69 (br, 2H), 1.92–1.90 (m, 8H), 1.66–1.57 (m, 2H), 1.50–1.48 (m, 2H), 1.29 (br, 8H). ^{13}C NMR (CDCl_3): δ 166.15, 158.26, 150.94, 149.61, 149.50, 147.25, 140.36, 128.43, 128.36, 128.28, 123.59, 122.92, 121.66, 120.09, 119.03, 115.68, 112.73, 110.18, 72.93, 68.13, 55.81, 49.35, 39.64, 33.87, 31.69, 29.62, 29.09, 26.74, 25.35, 24.74, 23.90, 23.01, 22.72. HRMS (ESI) m/z calcd for $\text{C}_{33}\text{H}_{46}\text{N}_4\text{O}_6$ [M^+] 618.3417; found 618.3422. Anal. Calcd for ($\text{C}_{33}\text{H}_{46}\text{N}_4\text{O}_6 \cdot \text{H}_2\text{O}$): found C, 65.91; H, 7.62; N, 8.75; requires C, 66.02; H, 7.60; N, 8.80.

6-{2-Methoxy-4-[(1E)-3-oxo-3-(8-(1,2,3,4-tetrahydroacridin-9-ylamino)octylamino)prop-1-enyl]phenoxy}hexyl Nitrate (3t). Compound **10e** (0.31 g, 1 mmol) reacted with compound **8d** (0.34 g, 1 mmol) to furnish **3t** as a yellow solid (0.21 g, 33%); mp 33–35 °C. ^1H NMR (CDCl_3): δ 7.97–7.89 (m, 2H), 7.57–7.51 (m, 2H), 7.36–7.30 (t, 1H), 7.04–7.00 (m, 2H), 6.82–6.79 (d, 1H), 6.30 (d, $J = 15.5$ Hz, 1H), 5.97–5.92 (t, 1H), 4.47–4.41 (t, 2H), 4.04–3.99 (t, 3H), 3.84 (s, 3H), 3.48 (br, 2H), 3.38–3.30 (m, 2H), 3.05 (br, 2H), 2.69 (br, 2H), 1.90 (br, 6H), 1.85–1.72 (m, 2H), 1.69–1.61 (m, 2H), 1.50 (br, 6H), 1.29 (br, 8H). ^{13}C NMR (CDCl_3): δ 166.17, 158.21, 150.98, 149.94, 149.41, 147.18, 140.53, 128.40, 127.90, 123.61, 122.92, 121.78, 120.05, 118.75, 115.64, 112.50, 110.13, 73.21, 68.63, 55.90, 49.36, 39.63, 33.83, 31.69, 29.63, 29.09, 28.83, 26.74, 26.65, 25.58, 25.42, 24.74, 23.01, 22.71. HRMS (ESI) m/z calcd for $\text{C}_{37}\text{H}_{50}\text{N}_4\text{O}_6$ [M^+] 646.3730; found 646.3735. Anal. Calcd for ($\text{C}_{37}\text{H}_{50}\text{N}_4\text{O}_6 \cdot \frac{1}{2}\text{H}_2\text{O}$): found C, 68.01; H, 8.16; N, 8.18; requires C, 67.76; H, 7.84; N, 8.54.

(E)-3-(3-Methoxy-4-propoxyphenyl)-N-[3-(1,2,3,4-tetrahydroacridin-9-ylamino)propyl]acrylamide (3u). Following general procedure V, compound **10b** (0.26 g, 1 mmol) reacted with compound **8e** (0.24 g, 1 mmol) to furnish **3u** as a yellow solid (0.17 g, 36%); mp 70–72 °C. ^1H NMR (CDCl_3): δ 8.06–8.03 (d, 1H, arom), 7.90–7.87 (d, 1H, arom), 7.59 (d, $J = 15.5$ Hz, 1H, COCH=CH), 7.55–7.49 (t, 1H, arom), 7.36–7.30 (t, 1H, arom), 7.04–6.96 (m, 2H, arom), 6.82–6.78 (d, 1H, arom), 6.55–6.50 (t, 1H, CONH), 6.32 (d, $J = 15.5$ Hz, 1H, COCH=CH), 5.02–4.96 (t, 1H, NH), 4.00–3.94 (t, 2H, OCH₂), 3.81 (s, 3H, OCH₃), 3.55–3.51 (m, 4H, NHCH₂CH₂CH₂NHCO), 3.03 (br, 2H, C4–H₂), 2.75 (br, 2H, C1–H₂), 1.89–1.81 (m, 8H, C2–H₂, C3–H₂, NHCH₂CH₂, OCH₂CH₂), 1.05–0.99 (t, 3H, OCH₂CH₂CH₃). ^{13}C NMR (CDCl_3): δ 167.13 (NHCO), 158.28 (arom), 150.72 (arom), 150.29 (arom), 149.43 (arom), 146.99 (arom), 141.10 (COCH=CH), 128.41 (arom), 128.22 (arom), 127.53 (arom), 123.82 (arom), 122.70 (arom), 121.95 (arom), 120.22 (COCH=CH), 118.19 (arom), 116.28 (arom), 112.48 (arom), 110.27 (arom), 70.44 (OCH₂), 55.96 (OCH₃), 45.30 (CH₂NHCO), 36.78 (NHCH₂), 33.78 (C4), 31.57 (NHCH₂CH₂), 25.13 (C1), 23.04 (C3), 22.69 (C2), 22.36 (OCH₂CH₂CH₃), 10.38 (OCH₂CH₂CH₃). HRMS (ESI) m/z calcd for $\text{C}_{29}\text{H}_{35}\text{N}_3\text{O}_3$ [M^+] 473.2678; found 473.2681. Anal. Calcd for ($\text{C}_{29}\text{H}_{35}\text{N}_3\text{O}_3 \cdot \frac{1}{2}\text{H}_2\text{O}$): found C, 72.03; H, 7.40; N, 8.46; requires C, 72.17; H, 7.52; N, 8.71.

(E)-3-(4-Hydroxy-3-methoxyphenyl)-N-[6-(1,2,3,4-tetrahydroacridin-9-ylamino)hexyl]acrylamide (4). Following general procedure V, compound **10d** (0.30 g, 1 mmol) reacted with ferulic acid (0.19 g, 1 mmol) to furnish **4** as a yellow solid (0.12 g, 25%); mp 172–174 °C. ^1H NMR ($\text{DMSO}-d_6$): δ 9.39 (br, 1H, OH), 8.11–8.08 (d, 1H, arom), 7.90–7.85 (t, 1H, arom), 7.70–7.66 (m, 1H, arom), 7.52–7.46 (m, 1H, arom), 7.35–7.25 (m, 2H, arom, COCH=CH),

7.09–7.08 (d, 1H, arom), 6.98–6.94 (m, 1H, arom), 6.78–6.75 (d, 1H, arom), 6.40 (d, $J = 15.5$ Hz, 1H, COCH=CH), 5.38–5.33 (t, 1H, CONH), 3.78 (s, 3H, OCH₃), 3.41–3.36 (m, 2H, NHCH₂), 3.15–3.07 (m, 2H, CH₂NHCO), 2.88–2.85 (m, 2H, C4–H₂), 2.72–2.79 (m, 2H, C1–H₂), 1.79–1.75 (m, 4H, C2–H₂, C3–H₂), 1.54–1.51 (m, 2H, NHCH₂CH₂), 1.41–1.36 (m, 2H, CH₂CH₂NHCO), 1.28–1.22 (m, 4H, NHCH₂CH₂CH₂CH₂). ^{13}C NMR ($\text{DMSO}-d_6$): δ 165.65 (NHCO), 158.41 (arom), 150.74 (arom), 148.63 (arom), 148.25 (arom), 147.41 (arom), 139.15 (COCH=CH), 128.78 (arom), 128.25 (arom), 126.90 (arom), 123.62 (arom), 123.47 (arom), 121.89 (arom), 120.76 (COCH=CH), 116.33 (arom), 116.09 (arom), 111.15 (arom), 55.96 (OCH₃), 48.37 (NHCH₂), 33.99 (CH₂NHCO), 31.04 (NHCH₂CH₂), 26.67 (CH₂CH₂NHCO), 26.51 (C4), 25.54 (C1, NHCH₂CH₂CH₂), 23.21 (NHCH₂CH₂CH₂CH₂), 22.92 (C3, C2). HRMS (ESI) m/z calcd for $\text{C}_{29}\text{H}_{35}\text{N}_3\text{O}_3$ [M^+] 473.2678; found 473.2674. Anal. Calcd for ($\text{C}_{29}\text{H}_{35}\text{N}_3\text{O}_3 \cdot \frac{1}{2}\text{H}_2\text{O}$): found C, 72.13; H, 7.71; N, 8.47; requires C, 72.17; H, 7.52; N, 8.71.

Cholinesterase Inhibition Assay in Vitro. The assay followed the method of Ellman et al.,³³ using a Shimadzu 160 spectrophotometer. AChE (EC3.1.1.7, Type VI–S, from Electric Eel) and BuChE (EC3.1.1.8, from equine serum), 5,5'-dithiobis(2-nitrobenzoic acid) (Ellman's reagent, DTNB), acetylthiocholine (ATC), and butyrylthiocholine (BTC) iodides were purchased from Sigma-Aldrich (Steinheim, Germany). AChE/BuChE stock solution was prepared by adjusting 500 units of the enzyme and 1 mL of gelatin solution (1% in water) to 100 mL with water. This enzyme solution was further diluted before use to give 2.5 units/mL in 1.4 mL aliquots. ATC/BTC iodide solution (0.075 M) was prepared in water. DTNB solution (0.01 M) was prepared in water containing 0.15% (w/v) sodium bicarbonate. For buffer preparation, potassium dihydrogen phosphate (1.36 g, 10 mmol) was dissolved in 100 mL of water and adjusted with KOH to pH = 8.0 ± 0.1. Stock solutions of the test compounds were prepared in ethanol, 100 μL of which gave a final concentration of 10^{-4} M when diluted to the final volume of 3.32 mL. For each compound, a dilution series of at least five different concentrations (normally 10^{-4} – 10^{-9} M) was prepared.

For measurement, a cuvette containing 3.0 mL of phosphate buffer, 100 μL of the respective enzyme, and 100 μL of the test compound solution was allowed to stand for 5 min before 100 μL of DTNB were added. The reaction was started by addition of 20 μL of the substrate solution (ATC/BTC). The solution was mixed immediately, and exactly 2 min after substrate addition the absorption was measured at 25 °C at 412 nm. For the reference value, 100 μL of water replaced the test compound solution. For determining the blank value, additionally 100 μL of water replaced the enzyme solution. Each concentration was measured in triplicate at 25 °C. The inhibition curve was obtained by plotting percentage enzyme activity (100% for the reference) versus logarithm of test compound concentration. Calculation of the IC_{50} values was performed with Graph Pad Prism 4.

Kinetic measurements were performed in the same manner, while the substrate (ATC/BTC) was used in concentrations of 25, 50, 90, 150, 226, and 452 μM for each test compound concentration and the reaction was extended to 4 min before measurement of the absorption. V_{max} and K_{m} values of the Michaelis–Menten kinetics were calculated by nonlinear regression from substrate–velocity curves using Graph Pad Prism 4. Linear regression was used for calculating the Lineweaver–Burk plots.

Detection of Nitrite (Griess Reaction). A solution of the appropriate compound (80 μL) in DMSO was added to 320 μL of phosphate buffer (pH 7.4) containing 5 mM L-cysteine. The final concentration of the compound was 10^{-4} M. After incubation for 1.5 h at 37 °C, 120 μL of the reaction mixture was treated with 25 μL of Griess reagent (2 g of sulfanilamide, 0.1 g of N-naphthylethylenediamine dihydrochloride, 85% phosphoric acid [5 mL] in distilled water [final volume, 50 mL]). After 30 min in darkness at room temperature, the absorbance was measured at 540 nm using a microplate reader TECAN Safire2 (Tecan Group Ltd, Maennedorf, Switzerland). Each compound was measured in triplicate. Standard sodium nitrite solutions (0, 0.01, 0.03, 0.05, 0.07, 0.09, 0.20, and 0.40 $\mu\text{g}/\text{mL}$)

were used to construct the calibration curve, from which the amount of nitric oxide release (quantitated as nitrite ion) was calculated.

Vascular Relaxation Study. Aortic rings isolated from rat heart (3–5 mm long) were suspended between two L-shaped platinum hooks and mounted under a passive tension (1–1.1 g) in a 10 mL organ bath filled with modified Krebs–Henseleit solution, which was kept at 37 °C. Preparation was connected to isometric force transducer JZ100 (New Channel Instruments, Gaobeidian, China). After an equilibration period of 60 min, contractions were induced by norepinephrine (NE, final concentration 10^{-5} M) to detect the activity of the vessel. Endothelial integrity was further assessed by the acetylcholine (10^{-5} M)-induced relaxation of NE-precontracted vessels. The ring segments were initially made to contract with KCl (60 mM) and subsequently with L-cysteine (10^{-3} M). The relaxation response to addition of test compounds was studied after the contractions became constant by constructing a cumulative concentration–response curve. Relaxation responses were expressed as a percentage of the KCl (60 mM)-induced contraction.

Behavioral Studies. The experiments were performed with adult male ICR mice (weighing 18–22 g), which were purchased from Comparative Medicine Centre, Yangzhou University (certificate no. 2023793). Scopolamine hydrobromide was obtained from Aladdin Reagents, Shanghai, China. Tacrine hydrochloride hydrate was purchased from BioTrend, Wangen, Switzerland.

Scopolamine (0.2 mg/100 g b wt) were dissolved in saline and administered intraperitoneally (ip) 5 min before the training trial. Tacrine was dissolved in CMC-Na solution (0.5 g CMC-Na in 100 mL distilled water) and 0.5 mg/100 g b wt, corresponding to 1.978 $\mu\text{mol}/100$ g b wt, were given in intragastric (id) administration 1 h before the training trial. The new substances were dissolved in CMC-Na solution and an equimolar dose corresponding to tacrine was administered id 1 h before the training trial. Mice were divided into six groups. (i) vehicle, (ii) scopolamine, (iii) compound **1b** plus scopolamine, (iv) compound **3f** plus scopolamine, (v) compound **3u** plus scopolamine, and (vi) tacrine plus scopolamine were given to each group, respectively.

The mice were subjected to the passive avoidance test by using a step-through passive avoidance apparatus for mice RD1105-RA-M-1 (Mice Doctor, Shanghai, China). The apparatus contained two symmetrical compartments, a dark and a light chamber, which were separated by a dark board that had a door near the floor. The grid floors of the dark chamber consisted of copper bars. To begin with, the dark compartment was electrified to generate low intensity foot shocks (0.4 mA). A trial of 300 s started as soon as one animal was gently put inside the light compartment, with the head facing away from the door. After entering to the dark compartment, the mouse would return to the light one. Afterward, the mouse would repeat the actions. The number of enterings from the light room to the dark room was recorded as the indication for short time learning ability. Besides, a transfer from light chamber into the dark chamber was recorded as transfer latency time (TLT in seconds). The first trial was for training, and the retention was tested by a second trial 24 h later, in which the shock was not delivered. The criterion for improvement of memory impairment was taken as significant increase in the TLT on the test compounds groups comparing to the scopolamine group in second trial.

Hepatotoxicity Studies. The experiments were carried out on adult male ICR mice (weighing 18–22 g), which were purchased from Comparative Medicine Centre, Yangzhou University (certificate no. 2023793). Tacrine hydrochloride hydrate (BioTrend, Wangen, Switzerland) was dissolved in CMC-Na solution (0.5 g CMC-Na in 100 mL of distilled water) and 3 mg/100 g b wt, corresponding to 11.86 $\mu\text{mol}/100$ g b wt, were given in id. Test compounds were dissolved in CMC-Na solution, and the equimolar dose corresponding to tacrine was administered id. Heparinized serum was obtained 8, 20, and 30 h after dosing from the retrobulbar plexus to determine aspartate aminotransferase (ASAT) and alanine aminotransferase (ALT) activity, two indicators of a liver damage, using routine methods.

Histology. Tacrine and tested compounds treated rats were sacrificed in ether anesthesia 30 h after dosing, and livers were harvested. Two 3 mm sections of each liver extending from the hilus to the margin of the left lateral lobe were immediately placed in 10% buffered formaldehyde, fixed for two days, and embedded together in one paraffin block. Subsequently, 5 μm sections were prepared from these paraffin blocks. Paraffin sections of each block were deparaffinated and stained with hematoxylin and eosin or by means of the periodic acid–Schiff procedure for glycogen.

Statistics. The number of animals investigated per group for the histological and biochemical investigations comprised $n = 3$ –12. For behavioral studies, 8–9 rats per group were used. Results are expressed as arithmetic means \pm SEM. For statistical analysis, Student's *t* test ($p \leq 0.05$) was applied.

Molecular Modeling. The docking study was performed by using CDOCKER module inbuilt in DS. CDOCKER was an in-house docking method as described previously.^{42,43} In general, CDOCKER generated ligand “seeds” to populate the binding pocket. Each seed was then subjected to high temperature molecular dynamics (MD) using a modified version of CHARMM force field. Each of the structures from the MD run were then located and fully minimized. The solutions were then clustered according to position and conformation and ranked by energy. CHARMM charges were used for the protein structure. The cocrystal structure of bis(7)-tacrine with *Torpedo California* AChE (TcAChE, PDB id: 2CKM) was selected for molecular modeling. Residues around bis(7)-tacrine in AChE (in 9 Å radius) was set as binding site. The heating step, cooling steps, and cooling temperature were set to 5000, 5000, and 310, respectively. Other parameters were kept as default. The MM/PBSA calculations were carried out by using “binding energy with MM/PBSA” protocol within Pipeline Pilot 8.0. All the parameters were kept as default.

■ ASSOCIATED CONTENT

📄 Supporting Information

Detailed synthetic procedures as well as physical, analytical, and spectral data for intermediary compounds. This material is available free of charge via the Internet at <http://pubs.acs.org>.

■ AUTHOR INFORMATION

Corresponding Author

*For H.L.: phone, +86-25-83271043; fax, +86-25-83271142; E-mail, hliao@cpu.edu.cn. For J.L.: phone, +49-3641949803; Fax, +49-3641949802; E-mail, j.lehmann@uni-jena.de. For Y.Z.: phone, +86-25-83271015; fax, +86-25-83271015; E-mail, zyhtgd@hotmail.com.

Notes

The authors declare no competing financial interest.

■ ACKNOWLEDGMENTS

The support of “DAAD Sandwich Program” Scholarship (April 2010 to March 2012) is very gratefully acknowledged. We thank the National Science Foundation of China (NSFC, no. 30973608), the National Natural Science Foundation of China (no. 81070967), and the Natural Science Foundation of Jiangsu Province of China (no. BK2009296) for funding. We also thank Yinquan Fang, Zhe Zhang, and Jianing Wang for their valuable help concerning this project.

■ ABBREVIATIONS USED

AD, Alzheimer's disease; ACh, acetylcholine; ChEs, cholinesterases; AChE, acetylcholinesterase; BuChE, butyrylcholinesterase; CAS, catalytic active site; PAS, peripheral anionic site; A β , β -amyloid; ChEIs, cholinesterase inhibitors; MTDLs, multi-target-directed ligands; NO, nitric oxide; DCC, dicyclohexylcarbodiimide; DMAP, 4-dimethylaminopyridine; DMF, di-

methylformamide; THF, tetrahydrofuran; ISDN, isosorbide dinitrate; TLT, transfer latency time; ASAT, aspartate aminotransferase; ALT, alanine aminotransferase; HE, hematoxylin and eosin

REFERENCES

- (1) Scarpini, E.; Scheltens, P.; Feldman, H. Treatment of Alzheimer's Disease: Current Status and New Perspectives. *Lancet Neurol.* **2003**, *2*, 539–547.
- (2) Perry, E. K.; Tomlinson, B. E.; Blessed, G.; Bergman, K.; Gibson, P. H.; Perry, R. H. Correlation of Cholinergic Abnormalities with Senile Plaques and Mental Test Scores in Senile Dementia. *Br. Med. J.* **1978**, *25*, 1457–1459.
- (3) Holzgrabe, U.; Kapková, P.; Alptüzün, V.; Scheiber, J.; Kugelmann, E. Targeting Acetylcholinesterase to Treat Neurodegeneration. *Expert Opin. Ther. Targets* **2007**, *11*, 161–179.
- (4) Sussman, J. L.; Harel, M.; Frolow, F.; Oefner, C.; Goldman, A. L.; L., T.; Silman, I. Atomic Structure of Acetylcholinesterase from *Torpedo californica*: A Prototypic Acetylcholine-Binding Protein. *Science* **1991**, *253*, 872–879.
- (5) Axelsen, P. H.; Harel, M.; Silman, I.; Sussman, J. L. Structure and Dynamics of the Active Site Gorge of Acetylcholinesterase: Synergistic Use of Molecular Dynamics Simulation and X-ray Crystallography. *Protein Sci.* **1994**, *3*, 188–197.
- (6) Muñoz-Ruiz, P.; Rubio, L.; García-Palmero, E.; Dorronsoro, I.; del Monte-Millán, M.; Valenzuela, R.; Usán, P.; de Austria, C.; Bartolini, M.; Andrisano, V.; Bidon-Chanal, A.; Orozco, M.; Luque, F. J.; Medina, M.; Martínez, A. Design, Synthesis, and Biological Evaluation of Dual Binding Site Acetylcholinesterase Inhibitors: New Disease-Modifying Agents for Alzheimer's Disease. *J. Med. Chem.* **2005**, *48*, 7223–7233.
- (7) Bourne, Y.; Taylor, P.; Radić, Z.; Marchot, P. Structural Insights into Ligand Interactions at the Acetylcholinesterase Peripheral Anionic Site. *EMBO J.* **2003**, *22*, 1–12.
- (8) Butini, S.; Campiani, G.; Borriello, M.; Gemma, S.; Panico, A.; Persico, M.; Catalanotti, B.; Ros, S.; Brindisi, M.; Agnusdei, M.; Fiorini, I.; Nacci, V.; Novellino, E.; Belinskaya, T.; Saxena, A.; Fattorusso, C. Exploiting Protein Fluctuations at the Active-Site Gorge of Human Cholinesterases: Further Optimization of the Design Strategy to Develop Extremely Potent Inhibitors. *J. Med. Chem.* **2008**, *51*, 3154–3170.
- (9) Bartolini, M.; Bertucci, C.; Cavrini, V.; Andrisano, V. β -Amyloid Aggregation Induced by Human Acetylcholinesterase: Inhibition Studies. *Biochem. Pharmacol.* **2003**, *65*, 407–416.
- (10) Alvarez, A.; Opazo, C.; Alarcón, R.; Garrido, J.; Inestrosa, N. C. Acetylcholinesterase Promotes the Aggregation of Amyloid-Beta-Peptide Fragments by Forming a Complex with the Growing Fibrils. *J. Mol. Biol.* **1997**, *272*, 348–361.
- (11) Inestrosa, N. C.; Sagal, J. P.; Colombres, M. Acetylcholinesterase Interaction with Alzheimer Amyloid Beta. *Subcell. Biochem.* **2005**, *38*, 299–317.
- (12) Saxena, A.; Redman, A. M.; Jiang, X.; Lockridge, B. P.; Doctor, B. P. Differences in Active Site Gorge Dimensions of Cholinesterases Revealed by Binding of Inhibitors to Human Butyrylcholinesterase. *Biochemistry* **1997**, *36*, 14642–14651.
- (13) Conejo-García, A.; Pisani, L.; del NÚñez, M. C.; Catto, M.; Nicolotti, O.; Leonetti, F.; Campos, J. M.; Gallo, M. A.; Espinosa, A.; Carotti, A. Homodimeric Bis-Quaternary Heterocyclic Ammonium Salts as Potent Acetyl- and Butyrylcholinesterase Inhibitors: A Systematic Investigation of the Influence of Linker and Cationic Heads over Affinity and Selectivity. *J. Med. Chem.* **2011**, *54*, 2627–2645.
- (14) Darvesh, S.; Hopkins, D. A.; Geula, C. Neurobiology of Butyrylcholinesterase. *Nature Rev. Neurosci.* **2003**, *4*, 131–138.
- (15) Arendt, T.; Brückner, M. K.; Lange, M.; Volker, B. Changes in Acetylcholinesterase and Butyrylcholinesterase in Alzheimer's Disease Resemble Embryonic Development—A Study of Molecular Forms. *Neurochem. Int.* **1992**, *21*, 381–396.
- (16) Chianella, C.; Gragnaniello, D.; Delsler, P. M.; Visentini, M. F.; Sette, E.; Tola, M. R.; Barbujani, G.; Fuselli, S. BCHE and CYP2D6 Genetic Variation in Alzheimer's Disease Patients Treated with Cholinesterase Inhibitors. *Eur. J. Clin. Pharmacol.* **2011**, *67*, 1147–1157.
- (17) Ballard, C. G. Advances in the Treatment of Alzheimer's Disease: Benefits of Dual Cholinesterase Inhibition. *Eur Neurol.* **2002**, *47*, 64–70.
- (18) Terry, A. V., Jr.; Buccafusco, J. J. The Cholinergic Hypothesis of Age and Alzheimer's Disease-Related Cognitive Deficits: Recent Challenges and Their Implications for Novel Drug Development. *J. Pharmacol. Exp. Ther.* **2003**, *306*, 821–827.
- (19) Youdim, M. B.; Buccafusco, J. J. Multifunctional Drugs for Various CNS Targets in the Treatment of Neurodegenerative Disorders. *Trends Pharmacol. Sci.* **2005**, *26*, 27–35.
- (20) Bolognesi, M. L.; Cavalli, A.; Valgimigli, L.; Bartolini, M.; Rosini, M.; Andrisano, V.; Recanatini, M.; Melchiorre, C. Multi-Target-Directed Drug Design Strategy: From a Dual Binding Site Acetylcholinesterase Inhibitor to a Trifunctional Compound Against Alzheimer's Disease. *J. Med. Chem.* **2007**, *50*, 6446–6449.
- (21) Tumiatti, V.; Milelli, A.; Minarini, A.; Rosini, M.; Bolognesi, M. L.; Micco, M.; Andrisano, V.; Bartolini, M.; Mancini, F.; Recanatini, M.; Cavalli, A.; Melchiorre, C. Structure–Activity Relationships of Acetylcholinesterase Noncovalent Inhibitors Based on a Polyamine Backbone. 4. Further Investigation on the Inner Spacer. *J. Med. Chem.* **2008**, *51*, 7308–7312.
- (22) Furchgott, R. F.; Zawadzki, J. V. The Obligatory Role of Endothelial Cells in the Relaxation of Arterial Smooth Muscle by Acetylcholine. *Nature* **1980**, *288*, 373–376.
- (23) Moncada, S.; Higgs, A. The L-Arginine-Nitric Oxide Pathway. *N. Engl. J. Med.* **1993**, *329*, 2002–2012.
- (24) Cooke, J. P.; Dzau, V. J. Nitric Oxide Synthase: Role in the Genesis of Vascular Disease. *Annu. Rev. Med.* **1997**, *48*, 489–509.
- (25) Faraci, F. M. Role of Endothelium-Derived Relaxing Factor in Cerebral Circulation: Large Arteries vs Microcirculation. *Am. J. Physiol.* **1991**, *261*, 1038–1042.
- (26) Megson, I. L.; Webb, D. J. Nitric Oxide Donor Drugs: Current Status and Future Trends. *Expert Opin. Invest. Drugs* **2002**, *11*, 587–601.
- (27) Thatcher, G. R. J.; Bennett, B. M.; Reynolds, J. N. Nitric Oxide Mimetic Molecules as Therapeutic Agents in Alzheimer's Disease. *Curr. Alzheimer Res.* **2005**, *2*, 171–182.
- (28) Fang, L.; Appenroth, D.; Decker, M.; Kiehnopf, M.; Lupp, A.; Peng, S. X.; Fleck, C.; Zhang, Y. H.; Lehmann, J. NO-Donating Tacrine Hybrid Compounds Improve Scopolamine-Induced Cognition Impairment and Show Less Hepatotoxicity. *J. Med. Chem.* **2008**, *51*, 7666–7669.
- (29) Schiefer, I. T.; Abdul-Hay, S.; Wang, H. L.; Vanni, M.; Qin, Z. H.; Thatcher, G. R. J. Inhibition of Amyloidogenesis by Nonsteroidal Anti-inflammatory Drugs and Their Hybrid Nitrates. *J. Med. Chem.* **2011**, *54*, 2293–2306.
- (30) Fang, L.; Kraus, B.; Lehmann, J.; Heilmann, J.; Zhang, Y. H.; Decker, M. Design and Synthesis of Tacrine–Ferulic Acid Hybrids as Multi-Potent Anti-Alzheimer Drug Candidates. *Bioorg. Med. Chem. Lett.* **2008**, *18*, 2905–2909.
- (31) Fang, L.; Appenroth, D.; Decker, M.; Kiehnopf, M.; Roegler, C.; Deufel, T.; Fleck, C.; Peng, S. X.; Zhang, Y. H.; Lehmann, J. Synthesis and Biological Evaluation of NO-Donor–Tacrine Hybrids as Hepatoprotective Anti-Alzheimer Drug Candidates. *J. Med. Chem.* **2008**, *51*, 713–716.
- (32) Carlier, P. R.; Han, Y. F.; Chow, E. S.-H.; Li, C.P.-L.; Wang, H.; Lieu, T. X.; Wong, H. S.; Pang, Y.-P. Evaluation of Short-Tether Bis-THA AChE Inhibitors. A Further Test of the Dual Binding Site Hypothesis. *Bioorg. Med. Chem.* **1999**, *7*, 351–357.
- (33) Ellman, G. L.; Courtney, K. D.; Andres, V., Jr.; Feather-Stone, R. M. A New and Rapid Colorimetric Determination of Acetylcholinesterase Activity. *Biochem. Pharmacol.* **1961**, *7*, 88–95.
- (34) Reddy, K. K.; Shanker, K. S.; Ravinder, T.; Prasad, R. B. N.; Kanjilal, S. Chemo-enzymatic Synthesis and Evaluation of Novel

Structured Phenolic Lipids as Potential Lipophilic Antioxidants. *Eur. J. Lipid Sci. Technol.* **2010**, *112*, 600–608.

(35) Sorba, G.; Medana, C.; Fruttero, R.; Cena, C.; Di Stilo, A.; Galli, U.; Gasco, A. Water Soluble Furoxan Derivatives as NO Prodrugs. *J. Med. Chem.* **1997**, *40*, 463–469.

(36) Das, A.; Kapoor, K.; Sayeepriyadarshini, A. T.; Dikshit, M.; Palit, G.; Nath, C. Immobilization Stress-Induced Changes in Brain Acetylcholinesterase Activity and Cognitive Function in Mice. *Pharmacol. Res.* **2000**, *42*, 213–217.

(37) Gracon, S. I.; Knapp, M. J.; Berghoff, W. G.; Pierce, M.; de Jong, R.; Lobbstaël, S. J.; Symons, J.; Dombey, S. L.; Luscombe, F. A.; Kraemer, D. Safety of Tacrine: Clinical Trials, Treatment IND, and Postmarketing Experience. *Alzheimer Dis. Assoc. Disord.* **1998**, *12*, 93–101.

(38) Liu, J.; Waalkes, M. P. Nitric Oxide and Chemically Induced Hepatotoxicity: Beneficial Effects of the Liver-Selective Nitric Oxide Donor, V-PYRRO/NO. *Toxicology* **2005**, *208*, 289–297.

(39) Futter, L. E.; al-Swayeh, O. A.; Moore, P. K. A Comparison of the Effect of Nitroparacetamol and Paracetamol on Liver Injury. *Br. J. Pharmacol.* **2001**, *132*, 10–12.

(40) Rydberg, E. H.; Brumshtein, B.; Greenblatt, H. M.; Wong, D. M.; Shaya, D.; Williams, L. D.; Carlier, P. R.; Pang, Y. P.; Silman, I.; Sussman, J. L. Complexes of Alkylene-Linked Tacrine Dimers with *Torpedo californica* Acetylcholinesterase Binding of Bis(5)-tacrine Produce a Dramatic Rearrangement in the Active-Site Gorge. *J. Med. Chem.* **2006**, *49*, 5491–5500.

(41) Bolea, I.; Juárez-Jiménez, J.; de los Ríos, C.; Chioua, M.; Pouplana, R.; Luque, F. J.; Unzeta, M.; Marco-Contelles, J.; Samadi, A. Synthesis, Biological Evaluation and Molecular Modeling of Donepezil and *N*-[(5-(Benzyloxy)-1-methyl-1*H*-indol-2-yl)methyl]-*N*-methyl-prop-2-yn-1-amine Hybrids as New Multipotent Cholinesterase/Monoamine Oxidase Inhibitors for the Treatment of Alzheimer's Disease. *J. Med. Chem.* **2011**, *54*, 8251–8270.

(42) Wu, G.; Robertson, D. H.; Brooks, C. L., III; Vieth, M. Detailed Analysis of Grid-Based Molecular Docking: A Case Study of CDOCKER-A CHARMM-Based MD Docking Algorithm. *J. Comput. Chem.* **2003**, *24*, 1549–1562.

(43) Sun, H. P.; Zhu, J.; Chen, Y. D.; Sun, Y.; Zhi, H. J.; Li, Hao.; You, Q. D. Docking Study and Three-Dimensional Quantitative Structure–Activity Relationship (3D-QSAR) Analyses and Novel Molecular Design of a Series of 4-Aminoquinazolines as Inhibitors of Aurora B Kinase. *Chin. J. Chem.* **2011**, *29*, 1785–1799.